NACA

RESEARCH MEMORANDUM

EFFECTS OF ANGLE OF ATTACK AND AIRFOIL PROFILE

ON THE TWO-DIMENSIONAL FLUTTER DERIVATIVES

FOR AIRFOILS OSCILLATING IN PITCH AT

HIGH SUBSONIC SPEEDS

By John A. Wyss and Raymond Herrera

Ames Aeronautical Laboratory
Moffett Field, Calif.

NATIONAL ADVISORY COMMITTEE
FOR AERONAUTICS

WASHINGTON
October 15, 1954

UNCLASSIFIED

NATIONAL ADVISORY COMMITTEE FOR AERONAUTICS

RESEARCH MEMORANDUM

EFFECTS OF ANGLE OF ATTACK AND AIRFOIL PROFILE

ON THE TWO-DIMENSIONAL FLUTTER DERIVATIVES

FOR AIRFOILS OSCILLATING IN PITCH AT

HIGH SUBSONIC SPEEDS

By John A. Wyss and Raymond Herrera

SUMMARY

Two-dimensional aerodynamic lift and moment flutter derivatives
are presented for moderate and high angles of attack for several airfoil
profiles varying in thickness and thickness distribution. The deriva-
tives were evaluated from data obtained by means of pressure cells for
models oscillating about the quarter-chord axis at mean angles of attack
of 4° and 8° (and for one model at 10°) for amplitudes of $\pm 1^\circ$, for fre-
quencies up to 40 cycles per second, and for a range of Mach numbers
including values which lead to either partially stalled or supercritical
flow. Reduced frequency varied from about 0.12 to 1.2 at $M = 0.2$, and
from 0.03 to 0.30 at $M = 0.86$. Reynolds number based on the airfoil
chord varied from 3 million to 8 million.

The results of the investigation indicate that the variables, angle
of attack, airfoil profile, reduced frequency, and Mach number, each have
significant effects which appear to be interdependent. In general, for
angles of attack below the beginning of stall, reasonable agreement was
obtained with theory except for the phase angles of the moment deriva-
tives. This exception was due to changes of the center of pressure to
a point ahead of the quarter chord. As a first approximation, the Mach
number for lift divergence can be correlated with the Mach number at
which large variations of the derivatives occurred. Since the Mach num-
ber for lift divergence decreases with increasing angle of attack, the
onset of large variations in the derivatives can be expected to occur at
a lower Mach number as the angle of attack is increased. In some cases,
the possibility of a single-degree-of-freedom torsional instability was
indicated by a change in sign of the torsional-damping parameter.
Although a reduction in airfoil thickness has been previously shown to
be beneficial at low angles of attack, a trend toward instability results

at moderate angles of attack. For airfoils of equal thickness a rear-
ward location of the point of maximum thickness appeared to increase
torsional stability.

INTRODUCTION

Several previous investigations have been concerned with the meas-
urement of oscillatory aerodynamic derivatives for airfoils at high
angles of attack or in the stall region. One of the most recent, and
probably the most comprehensive, of these investigations is the one
reported by Halfman, Johnson, and Haley (ref. 1). In that report, ear-
lier results such as those obtained by Bratt and Scruton (ref. 2), Bratt
and Wight (ref. 3), Halfman (ref. 4), and Bratt, Wight, and Chinneck
(ref. 5) are discussed and evaluated together with proposed theoretical
applications such as that by Victory (ref. 6). It was indicated that
the large number of important variables made an adequate prediction of
stall flutter far more difficult than the already complex classical case
at zero mean angle of attack, so that only the most general conclusions
could be drawn. These variables included airfoil shape, mean angle of
attack, amplitude of oscillation, frequency parameter, the location of
the rotational axis, and Reynolds number. Since previous investigations
were conducted at very low speeds, the effects of another variable,
Mach number, were necessarily omitted.

One purpose of this report, therefore, is to present two-dimensional
oscillatory lift and moment data for a range of Mach numbers including
values which lead to either partially stalled or supercritical flow.
Data obtained with the same series of airfoils for mean angles of attack
of 0° and 2° have previously been presented in reference 7 and, hence,
another purpose of this report is to present data for higher angles of
attack.

SYMBOLS

a   velocity of sound, ft/sec

b   wing semichord, ft

c_l dynamic section lift coefficient

c_m dynamic section moment coefficient about quarter point
        of chord

f   frequency of oscillation, cps

i	$\sqrt{-1}$
k	reduced frequency, $\dfrac{\omega b}{V}$
M	Mach number, $\dfrac{V}{a}$
M_α	oscillatory aerodynamic section moment on wing about axis of rotation, positive with leading edge up
M_{LD}	Mach number for lift divergence
P_α	oscillatory aerodynamic section lift on wing, positive upwards
q	free-stream dynamic pressure, lb/sq ft
V	free-stream velocity, ft/sec
α	oscillatory angular displacement (pitch) about axis of rotation, positive with leading edge up, radians
α_m	mean angle of attack about which oscillation takes place, deg
θ	phase angle between oscillatory moment and position α, positive for moment leading α, deg
φ	phase angle between oscillatory lift and position α, positive for lift leading α, deg
ω	circular frequency, $2\pi f$, radians/sec
$\left\lvert\dfrac{dc_l}{d\alpha}\right\rvert$	magnitude of dynamic lift-curve slope, $\left\lvert\dfrac{P_\alpha e^{-i\varphi}}{2bq\alpha}\right\rvert$, per radian
$\left\lvert\dfrac{dc_m}{d\alpha}\right\rvert$	magnitude of dynamic moment-curve slope, $\left\lvert\dfrac{M_\alpha e^{-i\theta}}{4b^2 q\alpha}\right\rvert$, per radian
$\dfrac{\left\lvert\dfrac{dc_m}{d\alpha}\right\rvert \sin\theta}{k}$	torsional damping parameter

APPARATUS AND METHOD

The models and associated apparatus have been described in references 7 and 8, and therefore only the more salient features are described here. The airfoils, each with a chord of 2 feet, had NACA 65A012, 65A008, 65A004, 2-008, and 877A008[1] profiles. In figure 1, the model profiles are illustrated to show the variation of thickness and thickness distribution. The NACA 65A008 airfoil is marked to indicate the location of the pressure cells. Model instrumentation consisted of 15 flush-type pressure cells and 15 pressure orifices along the midspan of each surface of each model. The pressure orifice adjacent to each pressure cell provided an internal reference pressure for that pressure cell. These orifices were also used in conjunction with a multiple mercury manometer to determine the time-average pressure distribution. In order that the internal reference pressure of the pressure cells would be essentially steady, about 50 feet of 1/16-inch tubing was used from the orifice to the manometer and back to the pressure cell.

The two-dimensional channel in the Ames 16-foot high-speed wind tunnel in which the models were oscillated and the drive system are illustrated in figure 2. The channel was 20 feet long and 16 feet high.

Sample oscillograph records, taken on 14-channel oscillographs, are presented in figure 3. The traces in the upper portion of each record indicate the difference between the oscillatory pressures on the upper and lower surface for several chord stations. The sum trace, which was the summation of the output of all cells and therefore proportional to the variation of lift force, and the output of an NACA slide-wire position transducer, proportional to the model angle of attack, were simultaneously recorded. Records were obtained with Mach number and mean angle of attack constant for frequencies from 4 to 40 cycles per second at intervals of 4 cycles per second, and for an amplitude of ±1°. The lift was evaluated from a 12-point harmonic analysis for each of three consecutive cycles of the sum trace. The pitching moment was evaluated from a 12-point harmonic analysis of the individual cell traces for one cycle.

In order to minimize tunnel-wall effects due to the phenomenon of wind-tunnel resonance (refs. 9, 10, and 11), all data obtained within 10 percent of the tunnel resonant frequency have been omitted. Although such a procedure does not mean tunnel-wall effects have been completely eliminated over the entire frequency range, it is felt that tunnel-wall effects are a small factor in the trends of the data. (See ref. 7.)

---

[1]The NACA 877A008 profile was derived from the NACA 847A110 profile by using the lower-surface coordinates for both upper and lower surfaces and then reducing the thickness ratio to 8 percent.

For a discussion of other factors influencing the precision of the data, the reader is referred to references 12 and 13. As in reference 13, it was necessary to correct the component of the derivatives in phase with position for the inertia forces due to acceleration of the pressure-cell diaphragms (determined from data obtained at various frequencies in still air). As one example, for the highest frequency of oscillation at 0.8 Mach number, the correction was 5 percent or less of the measured values.

RESULTS

The basic data obtained in the investigation are presented as a function of reduced frequency for constant Mach numbers in figures 4 through 9. Reduced frequency was chosen for the abscissa in order to ~~~t the data in the most useful, and perhaps the most familiar, form ~ aircraft designer.

Figures 4 and 5 contain the lift and moment derivatives, respectively, for a mean angle of attack of 4°, for the three models which vary in thickness - NACA 65A012, 65A008, and 65A004.

Figures 6 and 7 contain the respective lift and moment derivatives, also for a mean angle of attack of 4°, for the three models which vary in thickness distribution - NACA 2-008, 65A008, and 877A008.

Figures 8 and 9 contain the data for a mean angle of attack of 8° for the three latter models, and also for a mean angle of attack of 10° for the NACA 65A008 airfoil.

Since the same range of variables is not necessarily included in each figure, for clarification the mean angles of attack and the Mach numbers are tabulated as follows:

NACA airfoil	Mach number										
	0.2	0.3	0.4	0.5	0.59	0.68	0.73	0.79	0.83	0.86	0.87
65A012				4°	4°	4°	4°	4°			
65A008	10°	10°	8°	4°,8°	4°,8°	4°	4°	4°			
65A004				4°	4°	4°	4°	4°	4°		4°
2-008	8°	8°	4°,8°	4°,8°	4°	4°	4°	4°	4°		
877A008		8°	4°,8°	4°,8°	4°,8°	4°	4°	4°	4°	4°	

The theoretical curves shown in each figure were obtained by cross-plotting theoretical results given by Dietze for Mach numbers of 0, 0.5, 0.6, and 0.7 (ref. 14), by Minhinnick for M = 0.8 (ref. 15), and by

Nelson and Berman for M = 1.0 (ref. 16). Values at intermediate Mach
numbers were obtained by interpolation, but the errors due to fairings
are believed to be small.

DISCUSSION

The results of the investigation indicated that the four basic para-
meters, (1) reduced frequency, (2) airfoil profile, (3) Mach number, and
(4) angle of attack, each had important effects which were, expectedly,
interdependent or interrelated. For example, increasing angle of attack
so that the flow became separated, or increasing Mach number so that the
flow became supercritical, is already known to have large effects on
steady-state aerodynamic characteristics and would therefore be expected
to have large effects on the oscillatory aerodynamic characteristics.
The fundamental purpose of the present discussion, then, is to point out
the important effects of the two variables, angle of attack and airfoil
profile, on the oscillatory flutter derivatives, and to indicate how the
derivatives are affected by changes in Mach number and reduced frequency.

Introductory Illustrations

Before examining the basic data, it is desirable to provide two
specific illustrations of some of the effects of these variables in order
that the reader may have a better understanding of the fundamental causes
of the large variations of the results. The first illustration is con-
cerned with a discussion of several features already indicated in fig-
ure 3.

Effect of angle of attack and Mach number on oscillatory chordwise
pressures.- The sample records shown in figure 3 were selected for the
NACA 65A008 airfoil since it is intermediate in thickness and thickness
distribution, and is therefore considered the reference airfoil. In
figure 3(b) the relative smoothness of the individual traces for $\alpha_m = 4^\circ$
at M = 0.59 is apparent. The nonsinusoidal nature and large amplitude
of the trace representing the variation with time of the pressure differ-
ence between the upper and lower surface at 1.25-percent-chord station
can be attributed to a small supersonic region near the nose of the air-
foil. Time-average pressure distributions indicated that the local flow
became supercritical at this Mach number when the angle of attack was
greater than 2°. With an increase in angle of attack (fig. 3(a)), the
increase in the intensity of the shock wave and an increase in the degree
of separation of flow may be interpreted from the increase in the ampli-
tude of the trace deflections and the irregularity of the pressure fluc-
tuations at the leading edge. When the Mach number was increased from
0.59 to 0.79, at a mean angle of attack of 4° (fig. 3(c)), the rearward

movement of the shock wave was indicated by the large nonsinusoidal pressure fluctuations at the 35- and 45-percent-chord stations.

Thus, figure 3 is useful in pointing out the radical changes to the oscillatory pressures which occur when either angle of attack or Mach number is increased beyond those conditions for which the flow has become critical.

Since such flow conditions also result in changes to steady-state aerodynamic characteristics, it would appear that figure 3 admits the possibility of large changes to the oscillatory derivatives when the lift-curve slope is nonlinear due to flow separation in partial-stall conditions, or when the Mach number for steady-state lift divergence is exceeded. The large effects on the oscillatory derivatives, when the Mach number for lift divergence has been exceeded, have been indicated in reference 7 for mean angles of attack of 0° and 2°. The effects of nonlinear lift curves attributed to flow separation will be discussed in conjunction with figure 10.

<u>Effect of airfoil profile on steady-state aerodynamic characteristics.</u>- In figure 10 the aerodynamic characteristics of the three 8-percent-thick airfoils are presented for a Mach number of 0.40. The steady-state variation of lift as a function of angle of attack (determined by means of a multiple-tube mercury manometer) is indicated by the unflagged symbols. The flagged symbols for the NACA 65A008 airfoil are for data obtained by means of strain-gage balances. The small differences at the higher angles of attack would appear to indicate that end effects were probably very small inasmuch as the strain-gage outputs were proportional to the total wing area while pressure orifices indicated the wing loading only along the midspan. The dashed lines included in this figure indicate the variation of lift determined by means of pressure cells as the models were slowly oscillated at about 2 cycles per second through large angles of attack. The vertical bars in figure 10 indicate the mean angle of attack for which the high-angle-of-attack derivatives are presented in figures 8 and 9 for amplitudes of $\pm1^{\circ}$.

It appears that the data for unsteady and steady conditions in this figure are qualitatively related in that the hysteresis loop at the higher angles of attack for the unsteady case becomes larger where the lift curve for the steady case departs more from the linear. For the airfoil designed for high maximum lift coefficient, the NACA 2-008 airfoil, the lift curve remains linear to an angle of attack of about 10°, while for the other two models the lift curve breaks at about 6°. It is obvious that if each airfoil were oscillated about a mean angle of attack of 8°, indicated by the vertical bar on each curve, the flow condition for the NACA 65A008 and 877A008 airfoils would be quite dissimilar from that for the NACA 2-008 airfoil. It can also be noted that the effect of a finite frequency was to delay the break of the lift curve to a higher angle of attack. This point is best illustrated for the NACA 65A008 airfoil in

that the break for the unsteady case occurred at about an 8° angle of attack, compared to about 6° for the steady case. This figure illustrates the importance of airfoil profile at high angles of attack.

The lift-curve slopes at an angle of attack of 8°, obtained from the static data shown in figure 10, were plotted in figure 8(c) for $k = 0$. It can be seen that these values are consistent with the trends shown by the pressure-cell data for each of the three models although the values for the models differ greatly.

Aerodynamic Flutter Derivatives

Although a detailed examination of figures 4 through 9 reveals many minor variations in the trends of the data, there are several major variations from theory and large changes in the flutter derivatives due to the effects of reduced frequency, Mach number, or angle of attack. It is to the major variations that the remainder of the discussion is directed.

Effect of reduced frequency on moment derivative.- For a mean angle of attack of 4° at Mach numbers up to 0.68, the most striking variation from theory occurred in the moment derivatives. From figures 5(a) and 7(a) it can be noted that as reduced frequency decreased, the phase angles converged toward 0° (i.e., the moment vector approached being in phase with airfoil position) in contrast to a phase angle of 270° predicted by the theory. Also, the magnitude of the moment derivative appears to approach a finite value rather than zero as the frequency approaches zero. Extrapolation of the lift and moment derivatives to $k = 0$ indicates that the aerodynamic center of the oscillatory lift was thus ahead of the quarter-chord point a distance up to 5 percent of the chord. This position of the aerodynamic center was not anticipated by the theory for $k = 0$; however, it should be pointed out that the theory does predict a forward location of the center of pressure at low values of reduced frequency.

For the rotational axis located at the quarter-chord point, only the noncirculatory terms remain in the theoretical expressions; for other locations of the rotational axis, the circulatory terms are included. It is interesting to note that for a midchord axis of rotation the theoretical phase angles converge toward 360°, while for a leading-edge location, the theoretical phase angles converge toward 180°. Hence, the theory indicates a large shift in phase angle as the location of the rotational axis moves across the fixed location of the center of pressure. Conversely, one might expect a large shift in phase angle, if the center of pressure moves across a fixed location of the rotational axis.

Effect of Mach number on moment derivative.- A large shift in the moment-derivative phase angles for all reduced frequencies did occur as

Mach number was increased and can be seen in figures 5(d), 5(e), 5(f), 7(d), 7(e), and 7(f). To illustrate this effect more clearly, figures 11 and 12 have been prepared. In these figures, the derivatives and their accompanying phase angles have been plotted as a function of Mach number for several values of reduced frequency. Attention is first directed to figures 11(b) and 12(b), which contain the moment derivatives and phase angles. Figures 11(a) and 12(a) which contain the lift derivatives and phase angles will be discussed in a following section.

Examination of figures 11(b) and 12(b) indicates that the large phase shift of the moment derivative was an effect of compressibility, and that the Mach number at which the shift occurred was dependent on airfoil profile. Thickness distribution had a greater effect than airfoil thickness, in that the shift occurred at a higher Mach number as the location of maximum thickness was moved toward the trailing edge, but was nearly the same for the models which varied in thickness.

Correlation with Mach number for lift divergence.- The large shift of the phase angle can be related to the Mach number for lift divergence. The approximate Mach numbers for lift divergence determined for an angle of attack of 4° from pressure distributions measured by means of the pressure orifices and the multiple-tube mercury manometer were as follows:

NACA airfoil	M_{LD}
65A012	0.66
65A008	.69
65A004	.77
2-008	.65
877A008	.72

Examination of figures 11(b) and 12(b) indicates that the large shift in the phase angle of the moment derivative occurred at Mach numbers greater than those for lift divergence. Moreover, it can be noted that the Mach number at which large reductions occurred in the magnitude of the lift derivative also were greater than the Mach number for lift divergence (figs. 11(a) and 12(a)). It therefore appears that a qualitative result of the present investigation is that the Mach number for lift divergence may be used (as a first approximation) as a criterion which is indicative of the onset of a large variation of the lift and moment derivatives as Mach number is increased. It might be noted that this result for 4° is similar to that found for mean angles of attack of 0° and 2° in reference 7. At the higher angles of attack, insufficient data were obtained to evaluate this criterion. However, since the Mach number for lift divergence decreases with increasing angle of attack, the onset of large variations in the flutter derivatives would be expected to occur at a lower Mach number as the angle of attack is increased.

Effect of thickness distribution at high angles of attack.- At a
Mach number of 0.2 (fig. 8(a)), for the airfoil designed for high maximum
lift coefficient (the NACA 2-008 airfoil), the lift derivatives and phase
angles are in noteworthy agreement with theory, except for a slight
increase in magnitude and a lag of the phase angle at the higher values
of reduced frequency. However, these exceptions at the higher reduced
frequencies appear to be characteristic of nearly all the data. At a
Mach number of 0.5 (fig. 8(d)), the effects of thickness distribution no
longer appear important. The trends of the results for each model are
nearly the same, with no apparent relation with theory. This result can
be attributed to leading-edge effects, since the flow over the leading
edge was supercritical at this Mach number for all three airfoils. As
Mach number is increased to 0.6 (fig. 8(e)), the variation with reduced
frequency becomes more pronounced for the 65A008 and 877A008 airfoils,
with a large increase in lift derivative as reduced frequency increases,
along with phase angles which lead the theoretical values except at the
highest reduced frequencies.

Effect of angle of attack at constant Mach number.- In order to
indicate the effects of increasing the mean angle of attack at a constant
Mach number, figure 13 has been prepared for the reference model at a
Mach number of 0.59 as a typical representation of the effects of angle
of attack. The data for 0° and 2° have been taken from table II of
reference 8.

In figure 13(a), there is little change in the variation of phase
angle and lift derivative up to a mean angle of attack of 4°. At
$\alpha_m = 8°$, the magnitude of the lift derivative varies much more markedly
with reduced frequency as previously discussed, along with a shift toward
a leading phase angle.

In figure 13(b), the shift at $\alpha_m = 8°$ of the phase angle to a
leading one, that is, $0° < \theta < 180°$, is of particular importance in that
the aerodynamic torsional damping of the airfoil is negative and there-
fore indicates the possibility of a single-degree-of-freedom type of
flutter which does not exist at the smaller angles of attack.

Torsional Damping with Relation to Stall Flutter

The large change in phase angle in figure 13(b) is an indication of
large changes of the torsional damping inasmuch as torsional damping
corresponds to that component of the moment in phase with velocity. Thus,
as the moment derivative passes through 180°, the torsional damping com-
ponent decreases to zero and becomes positive. Such conditions are also
indicated in figures 5(e) and 5(f) for the NACA 65A004 airfoil at
$\alpha_m = 4°$, and in figure 9 for the NACA 65A008 and 877A008 airfoils.

A reduction in torsional damping, even without a change in sign, has been found important in stall-flutter analysis by Victory in reference 6. It is therefore important that the results of the present investigation be examined with respect to the torsional-damping parameter. These results are summarized in figures 14 and 15. It might be noted that this parameter differs only by a constant from j_a used by Victory, and is equivalent to $m_{\dot{\theta}}$ used in British notation. It is also equivalent to the expression $c_{mq} + c_{m\dot{\alpha}}$ used in dynamic-stability notation.

It is first necessary to point out that for an axis of rotation at the quarter-chord point, at least for the incompressible case, the torsional damping is only a function of reduced frequency. For the speed range of the present investigation, the departure of the theory from linearity was small up to the largest reduced frequency. In view of this linearity, a torsional-damping parameter may be defined as a theoretical constant (for all frequencies) obtained by dividing the component of the moment derivative in phase with velocity by the reduced frequency. The torsional-damping parameter was examined at constant reduced frequencies as a function of Mach number. It was found that although there were variations with reduced frequency at each Mach number, the general trends with Mach number were similar in that the trends were primarily due to the effects of compressibility or separated flow rather than reduced frequency. It thus appeared that an average value at each Mach number would be representative of the general trends with Mach number. The average deviation from the theoretical constant can then be determined by a simple averaging process of the values for several different frequencies. It is in this manner that frequency has been removed as a parameter in figures 14 and 15.

Although large effects of reduced frequency have been shown, the averaging process in these figures is believed to be valid since for almost every case the models were oscillated through the same range of frequencies, except for the NACA 65A004 airfoil at a mean angle of attack of 4° for which data were taken only at frequencies up to 20 cycles per second. Data for 0° mean angle of attack are also included from reference 7 to illustrate better the reduction in Mach number at which large changes occurred as mean angle of attack was increased.

Effects of airfoil thickness on the torsional-damping parameter for various angles of attack.- These effects are summarized in figure 14. This figure indicates that, although a reduction in thickness appears favorable at 0° mean angle of attack, such is not necessarily the case at a 4° mean angle of attack insofar as the NACA 65A004 airfoil became abruptly unstable at M = 0.83. No comparison can be made at higher angles of attack, since data were not available for the 4- and 12-percent-thick airfoils. However, increasing the mean angle of attack from 8° to 10° resulted in a reduction in Mach number at which instability occurred for the reference airfoil.

Effects of thickness distribution for various angles of attack.-
These effects are summarized in figure 15. It is interesting to note the
changes to the torsional-damping parameter as the location of maximum
thickness moved toward the trailing edge. The NACA 2-008 airfoil became
abruptly unstable at 0° but not at the higher angles, although there was
a trend toward reduction of the torsional-damping parameter at 8°. In
contrast, the NACA 65A008 airfoil became unstable at 8° and 10°, had a
trend toward instability at 4°, but remained stable at 0°. On the other
hand, the airfoil with the most rearward location of maximum thickness,
the NACA 877A008 airfoil, had the greatest degree of stability at each
angle of attack. It would therefore appear that a rearward location of
the point of maximum thickness is most favorable from the standpoint of
single-degree-of-freedom flutter in a torsional mode.

CONCLUDING REMARKS

The results of the investigation indicate that the variables, reduced
frequency, airfoil profile, Mach number, and angle of attack, each have
significant effects which appear to be interdependent.

In general, for angles of attack below the beginning of stall, rea-
sonable agreement was obtained with theory except for the moment deriva-
tives. This exception was due to changes of the location of the center
of pressure to a point ahead of the quarter chord.

As a first approximation, the Mach number for lift divergence can be
correlated with the Mach number at which large variations of the deriva-
tives occurred. Since the Mach number for lift divergence decreases with
increasing angle of attack, the onset of large variations in the deriva-
tives can be expected to occur at a lower Mach number as the angle of
attack is increased.

In some cases, the possibility of a single-degree-of-freedom tor-
sional instability was indicated by a change in sign of the torsional-
damping parameter.

At small angles a reduction in airfoil thickness appears beneficial
since a trend toward instability did not occur for the NACA 65A004 airfoil
at 0°; however, at 4° angle of attack, a trend toward instability results
from decreasing airfoil thickness. For airfoils of equal thickness, a
rearward location of the point of maximum thickness appears to increase
torsional stability.

Ames Aeronautical Laboratory
    National Advisory Committee for Aeronautics
        Moffett Field, Calif., Aug. 12, 1954

REFERENCES

1. Halfman, Robert L., Johnson, H. C., and Haley, S. M.: Evaluation
    of High-Angle-of-Attack Aerodynamic-Derivative Data and Stall-
    Flutter Prediction Techniques. NACA TN 2533, 1951.

2. Bratt, J. B., and Scruton, C.: Measurements of Pitching Moment
    Derivatives for an Aerofoil Oscillating about the Half-Chord Axis.
    R. & M. No. 1921, British A.R.C., Nov. 1938.

3. Bratt, J. B., and Wight, K. C.: The Effect of Mean Incidence,
    Amplitude of Oscillation, Profile and Aspect Ratio on Pitching
    Moment Derivatives. R. & M. No. 2064, British A.R.C., June, 1945.

4. Halfman, Robert L.: Experimental Aerodynamic Derivatives of a
    Sinusoidally Oscillating Airfoil in Two-Dimensional Flow. NACA
    Rep. 1108, 1952. (Supersedes NACA TN 2465)

5. Bratt, J. B., Wight, K. C., and Chinneck, A.: Free Oscillations of
    an Aerofoil about the Half-Chord Axis at High Incidences, and
    Pitching Moment Derivatives for Decaying Oscillations. R. & M.
    No. 2214, British A.R.C., Sept. 1940.

6. Victory, Mary: Flutter at High Incidence. R. & M. No. 2048, British
    A.R.C., Jan. 1943.

7. Wyss, John A., and Monfort, James C.: Effects of Airfoil Profile on
    the Two-Dimensional Flutter Derivatives for Wings Oscillating in
    Pitch at High Subsonic Speeds. NACA RM A54C24, 1954.

8. Coe, Charles F., and Mellenthin, Jack A.: Buffeting Forces on Two-
    Dimensional Airfoils as Affected by Thickness and Thickness Dis-
    tribution. NACA RM A53K24, 1953.

9. Runyan, Harry L., and Watkins, Charles E.: Considerations on the
    Effect of Wind-Tunnel Walls on Oscillating Air Forces for Two-
    Dimensional Subsonic Compressible Flow. NACA TN 2552, 1951.

10. Runyan, Harry L., Woolston, Donald S., and Rainey, A. Gerald: A
    Theoretical and Experimental Study of Wind-Tunnel-Wall Effects on
    Oscillating Air Forces for Two-Dimensional Subsonic Compressible
    Flow. NACA RM L52I17a, 1953.

11. Woolston, Donald S., and Runyan, Harry L.: Some Considerations on
    the Air Forces on a Wing Oscillating Between Two Walls for Sub-
    sonic Compressible Flow. IAS Preprint No. 446, 1954.

12. Erickson, Albert L., and Robinson, Robert C.: Some Preliminary
    Results in the Determination of Aerodynamic Derivatives of Control
    Surfaces in the Transonic Speed Range by Means of a Flush-Type
    Electrical Pressure Cell. NACA RM A8H03, 1948.

13. Wyss, John A., and Sorenson, Robert M.: An Investigation of the
    Control-Surface Flutter Derivatives of an NACA 65_1-213 Airfoil in
    the Ames 16-Foot High-Speed Wind Tunnel. NACA RM A51J10, 1951.

14. Dietze, F.: The Air Forces of the Harmonically Vibrating Wing in a
    Compressible Medium at Subsonic Velocity (Plane Problem). Trans-
    lation No. F-TS-506-RE, Air Materiel Command, U. S. Army Air
    Forces, Nov., 1946; Part II: Numerical Tables and Curves. Trans-
    lation No. F-TS-948-RE, Air Materiel Command, U. S. Air Force,
    March, 1947.

15. Minhinnick, I. T.: Subsonic Aerodynamic Flutter Derivatives for
    Wings and Control Surfaces (Compressible and Incompressible Flow).
    Rep. No. Structures 87, British R.A.E., July, 1950.

16. Nelson, Herbert C., and Berman, Julian H.: Calculation on the Forces
    and Moments for an Oscillating Wing-Aileron Combination in Two-
    Dimensional Potential Flow at Sonic Speed. NACA Rep. 1128, 1953.
    (Supersedes NACA TN 2590)

NACA 65A012

NACA 2-008   NACA 65A008   NACA 877A008
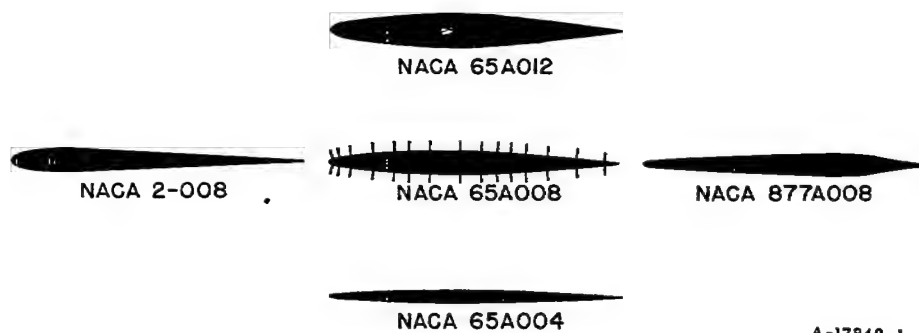
NACA 65A004   A-17840-1

MODEL PRESSURE-CELL LOCATIONS
[In Percent of Model Chord]

Cell number upper and lower surface	65A012 and 65A008	65A004 2-008, and 877A008
1	1.25	1.25
2	3.75	3.75
3	7.5	7.5
4	15	15
5	22.5	22.5
6	27.5	27.5
7	35	35
8	45	45
9	52.5	52.5
10	57.5	57.5
11	62.5	62.5
12	67.5	67.5
13	75	75
14	85	85
15	95	90

Figure 1.- Section profiles and pressure-cell locations of models.

DIAGRAMMATIC SKETCH OF WING DRIVE SYSTEM

OSCILLATOR

DRIVE MOTOR

TUNNEL WALL

AXIS OF ROTATION

TUNNEL WALL

A-14566

A-17840-3

(a) Downstream view.
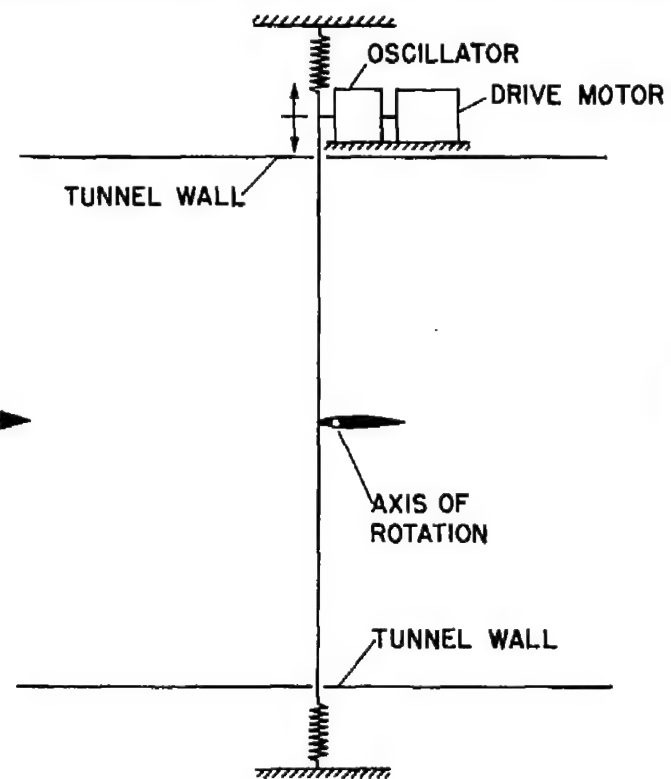
(b) Drive system.

Figure 2.- View of test section with model in place and diagrammatic sketch of drive system.
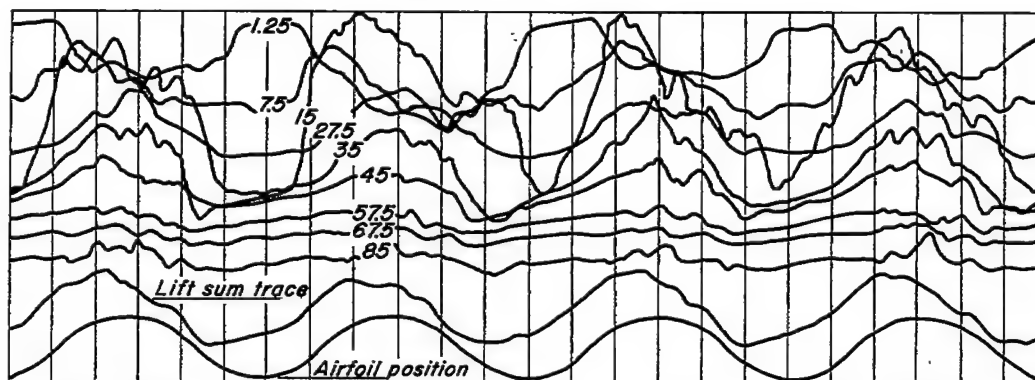
(a) Airfoil oscillating at 8° mean angle of attack, f=16.26 cps, M=0.59.

%c
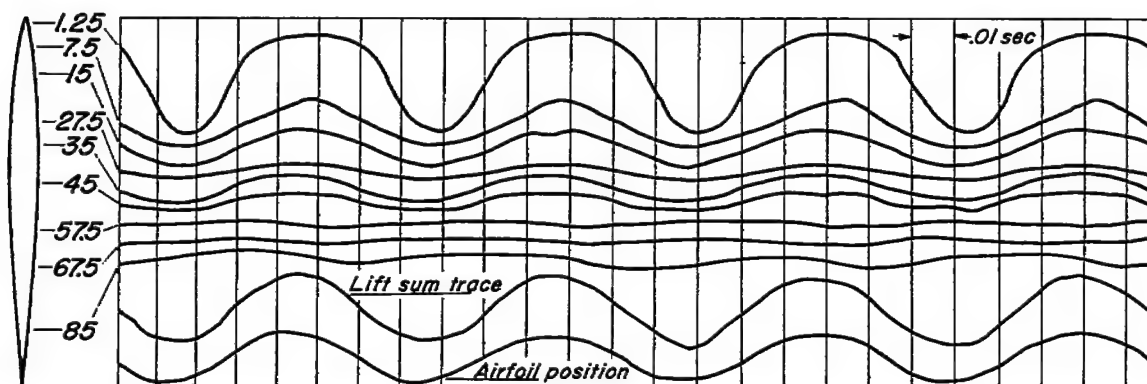
(b) Airfoil oscillating at 4° mean angle of attack, f=16.26 cps, M=0.59.
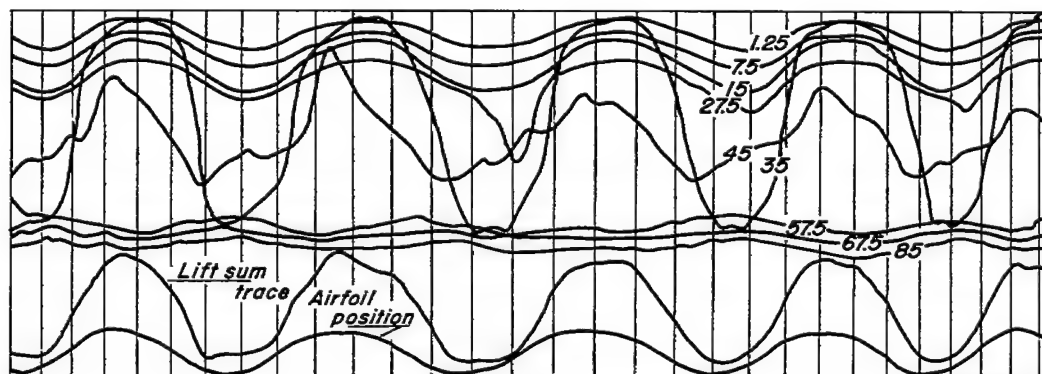
(c) Airfoil oscillating at 4° mean angle of attack, f=16.13 cps, M=0.79.

Figure 3.- Sample oscillograph records obtained for the NACA 65A008 airfoil.
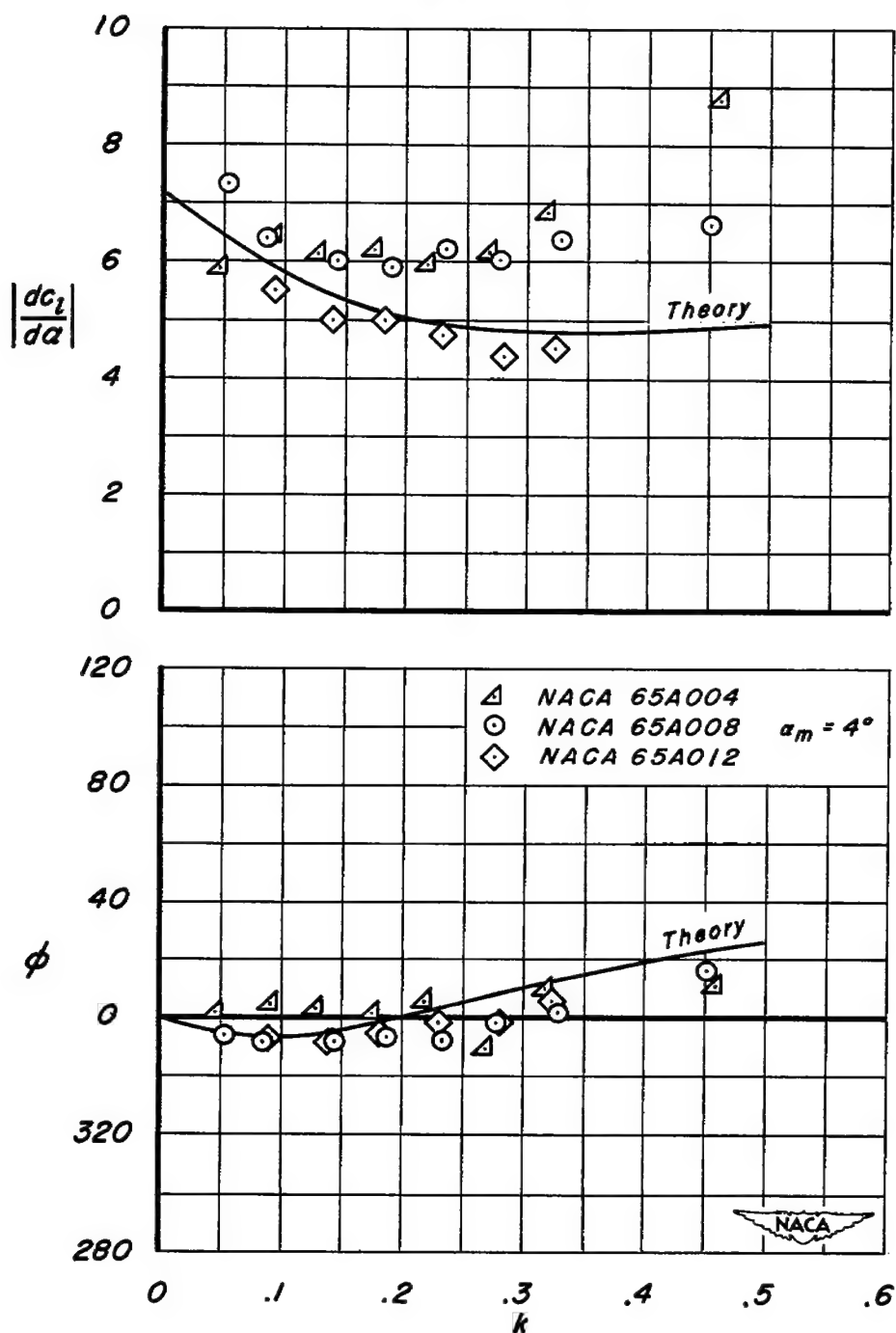
(a) Lift derivative and phase angle as a function of
reduced frequency. M = 0.49.

Figure 4.- Effects of airfoil thickness on lift flutter
derivative and phase angle.
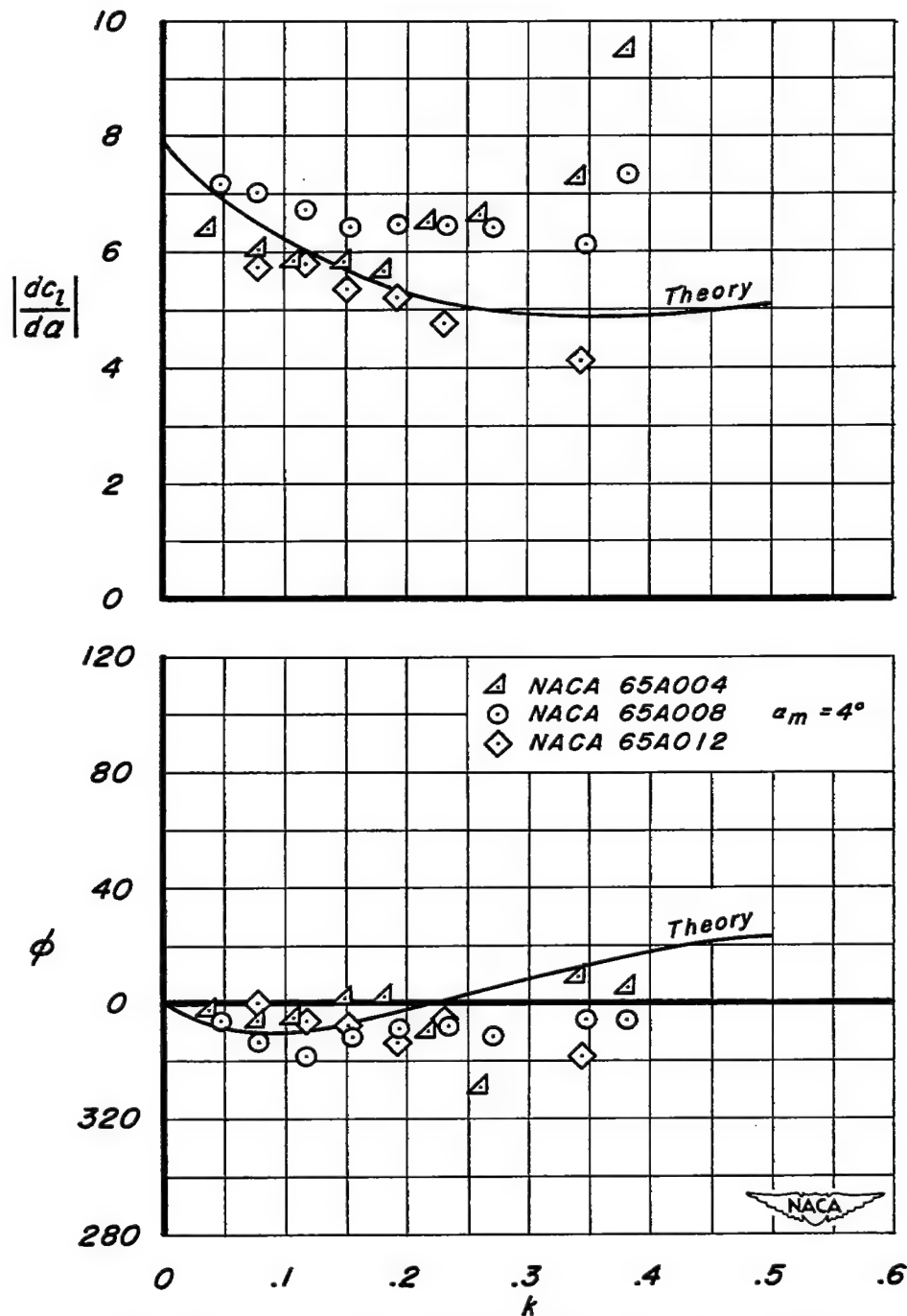
(b) Lift derivative and phase angle as a function of
reduced frequency. M = 0.59.

Figure 4.- Continued.
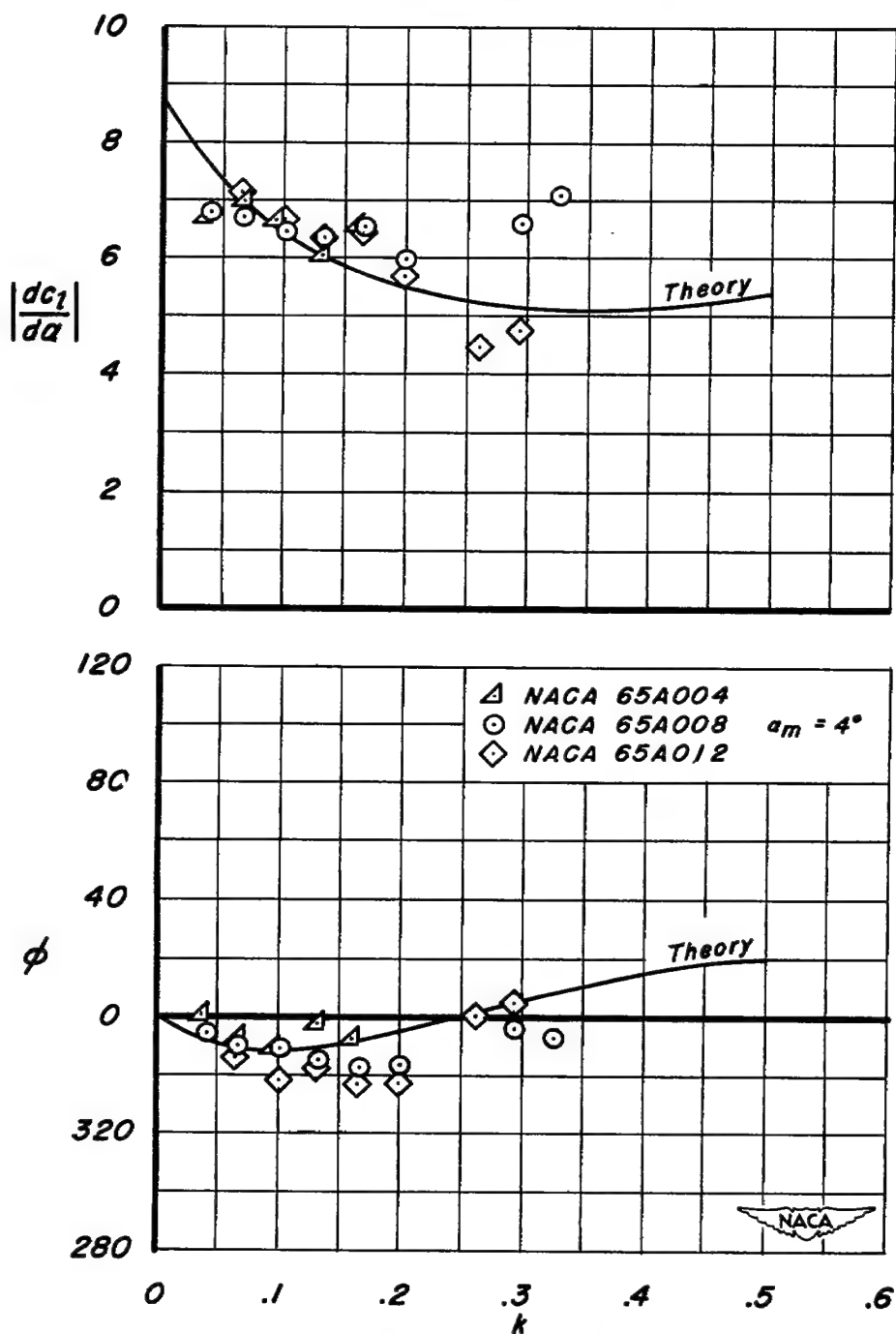
(c) Lift derivative and phase angle as a function of
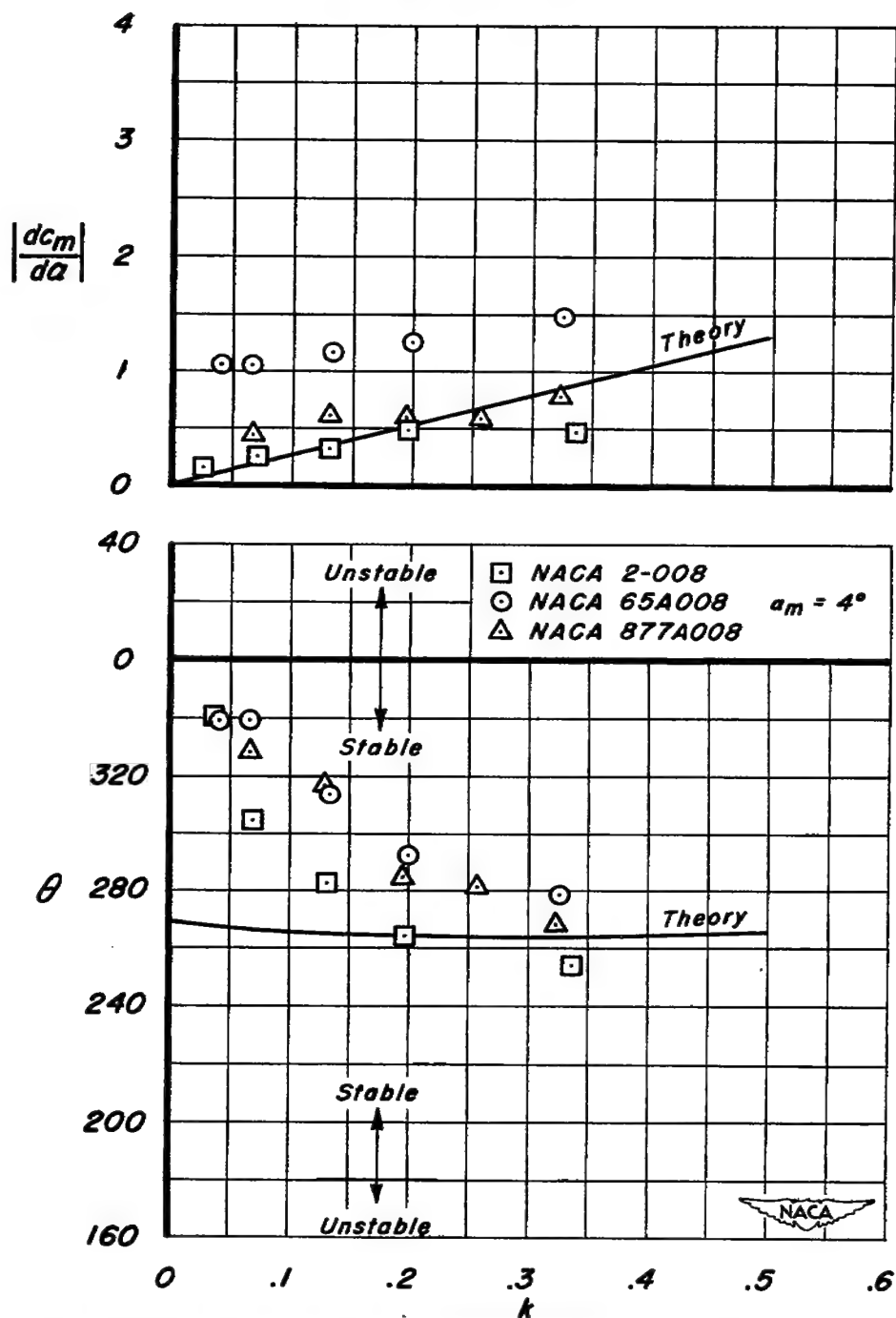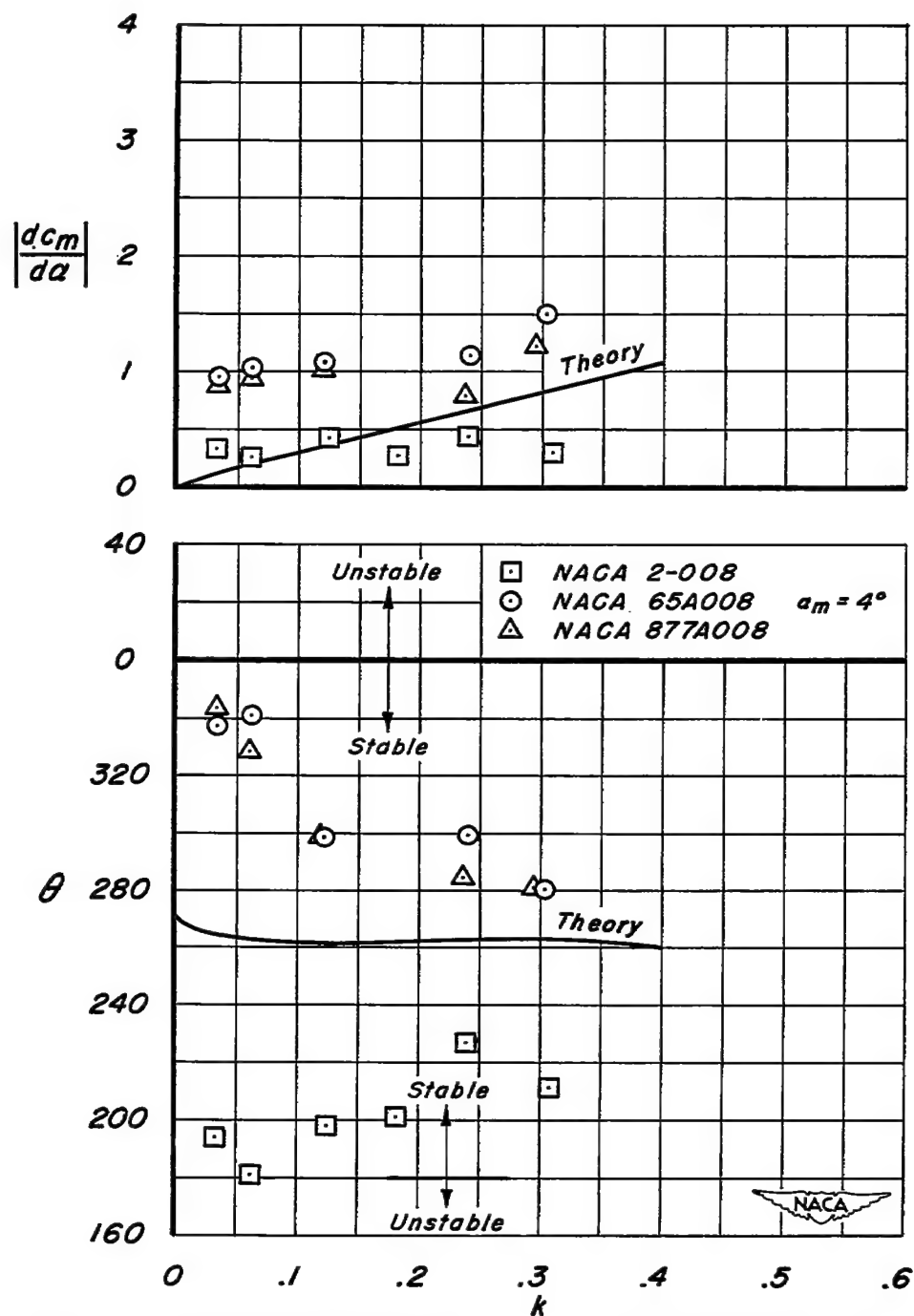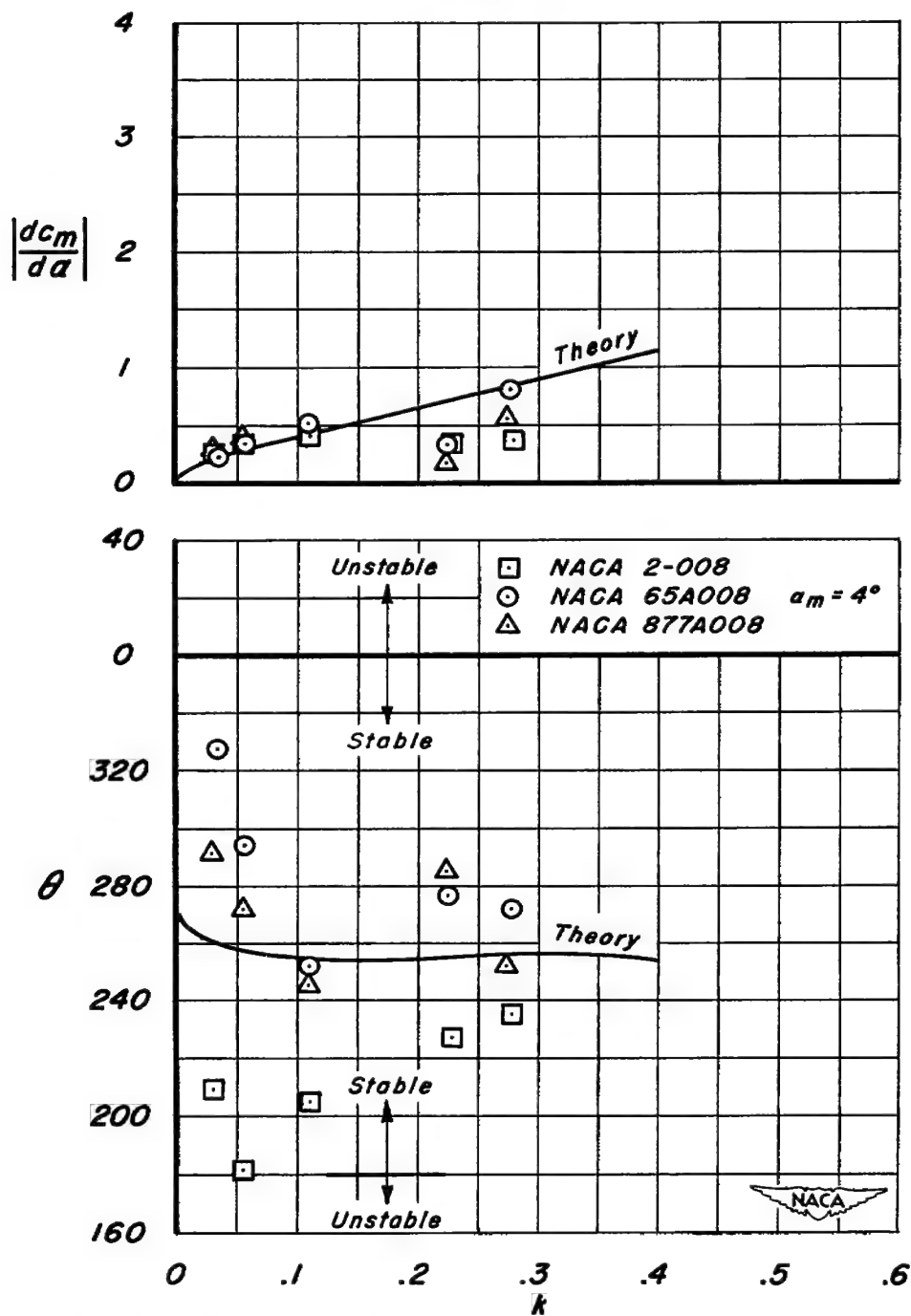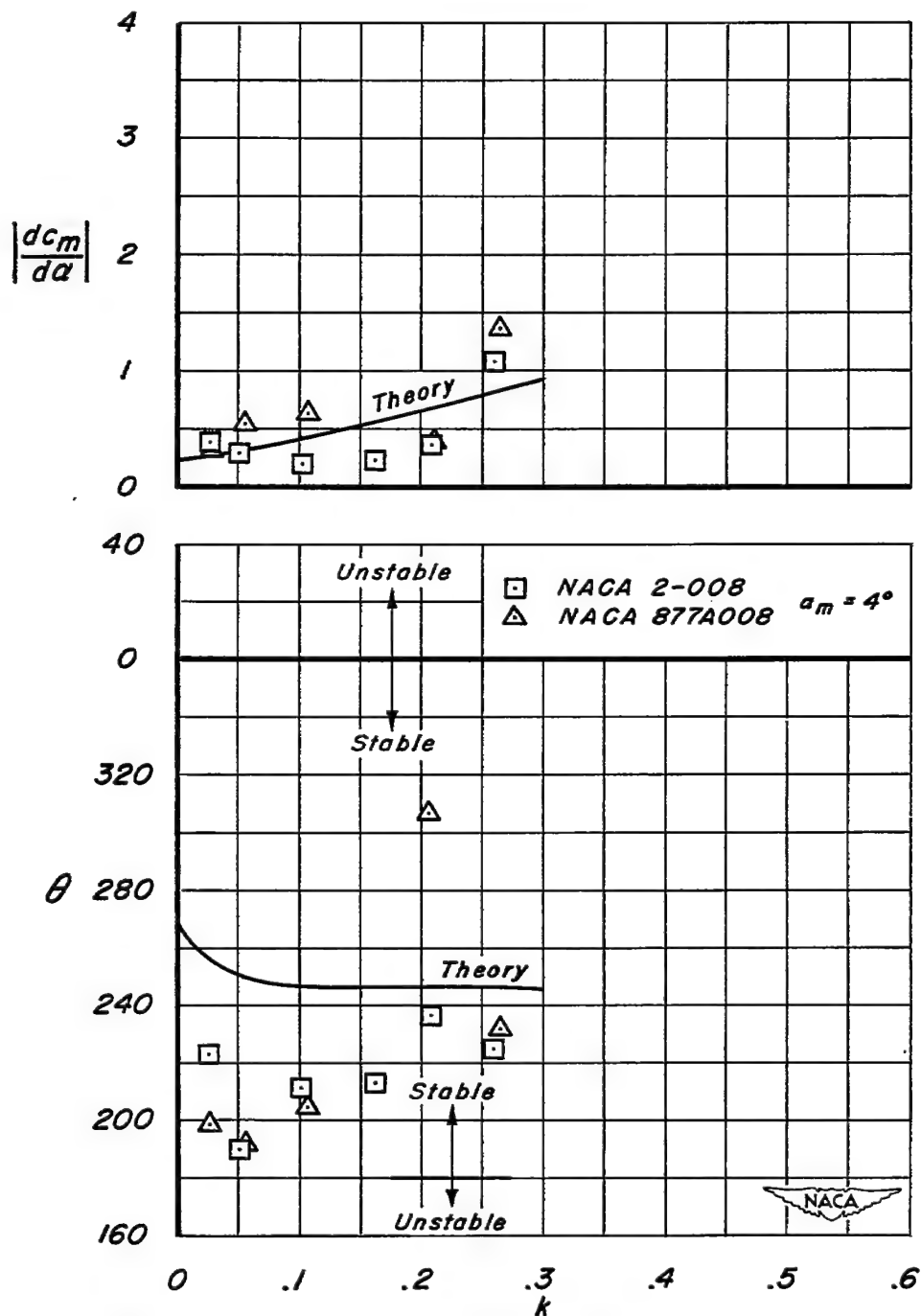reduced frequency. M = 0.68.

Figure 4.- Continued.
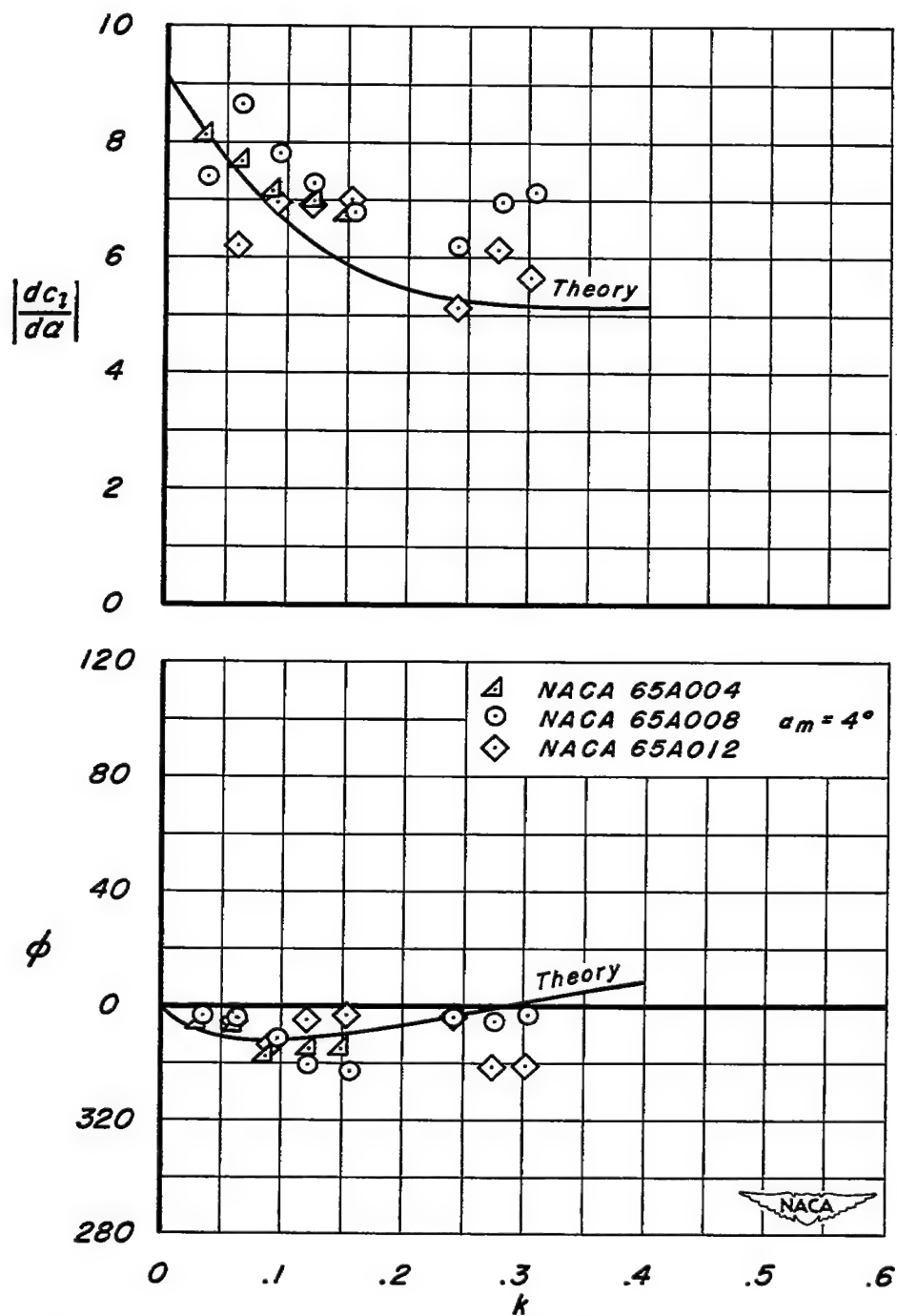
(d) Lift derivative and phase angle as a function of
reduced frequency. M = 0.73.

Figure 4.- Continued.
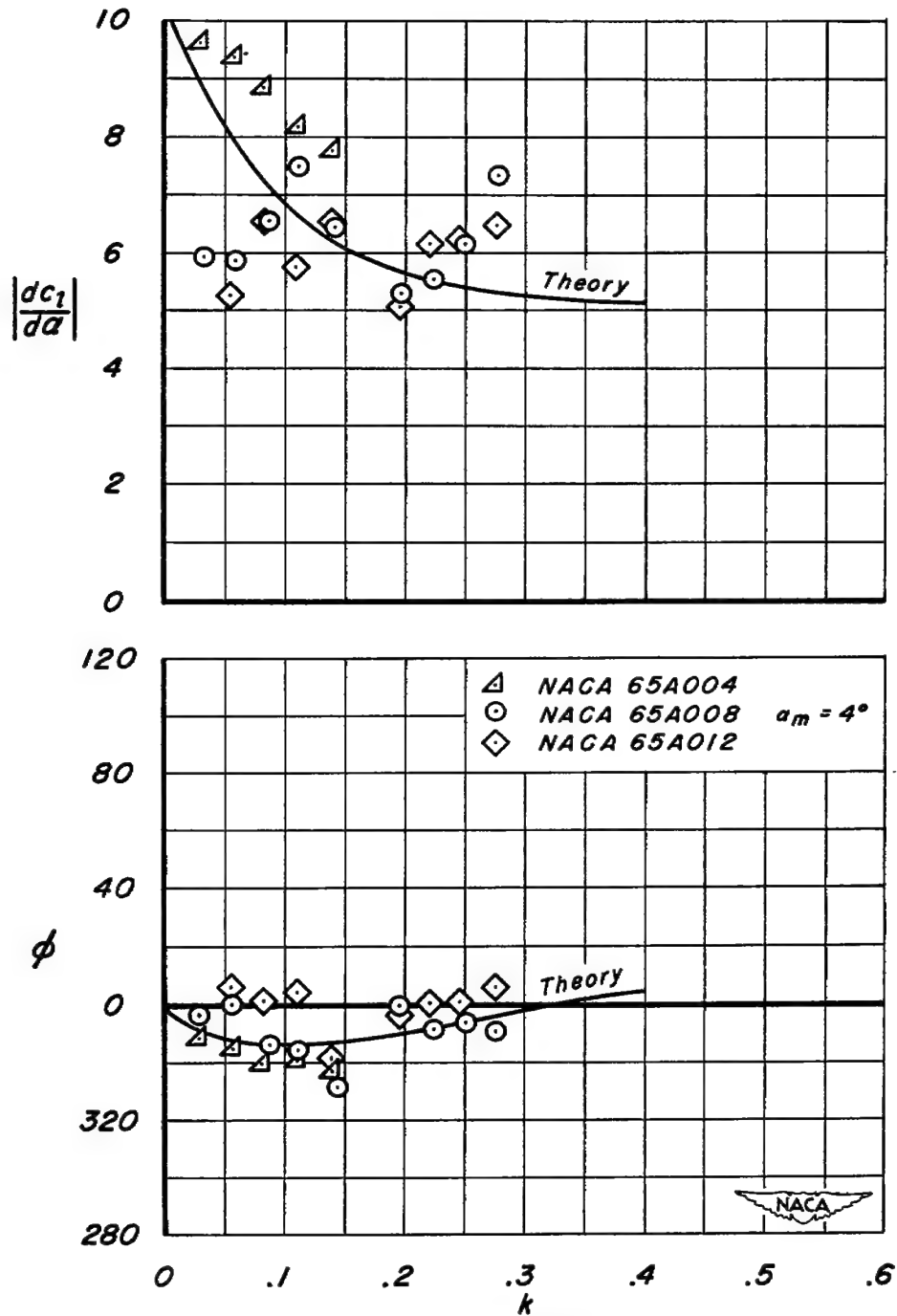
(e) Lift derivative and phase angle as a function of
reduced frequency. M = 0.79.
Figure 4.- Continued.
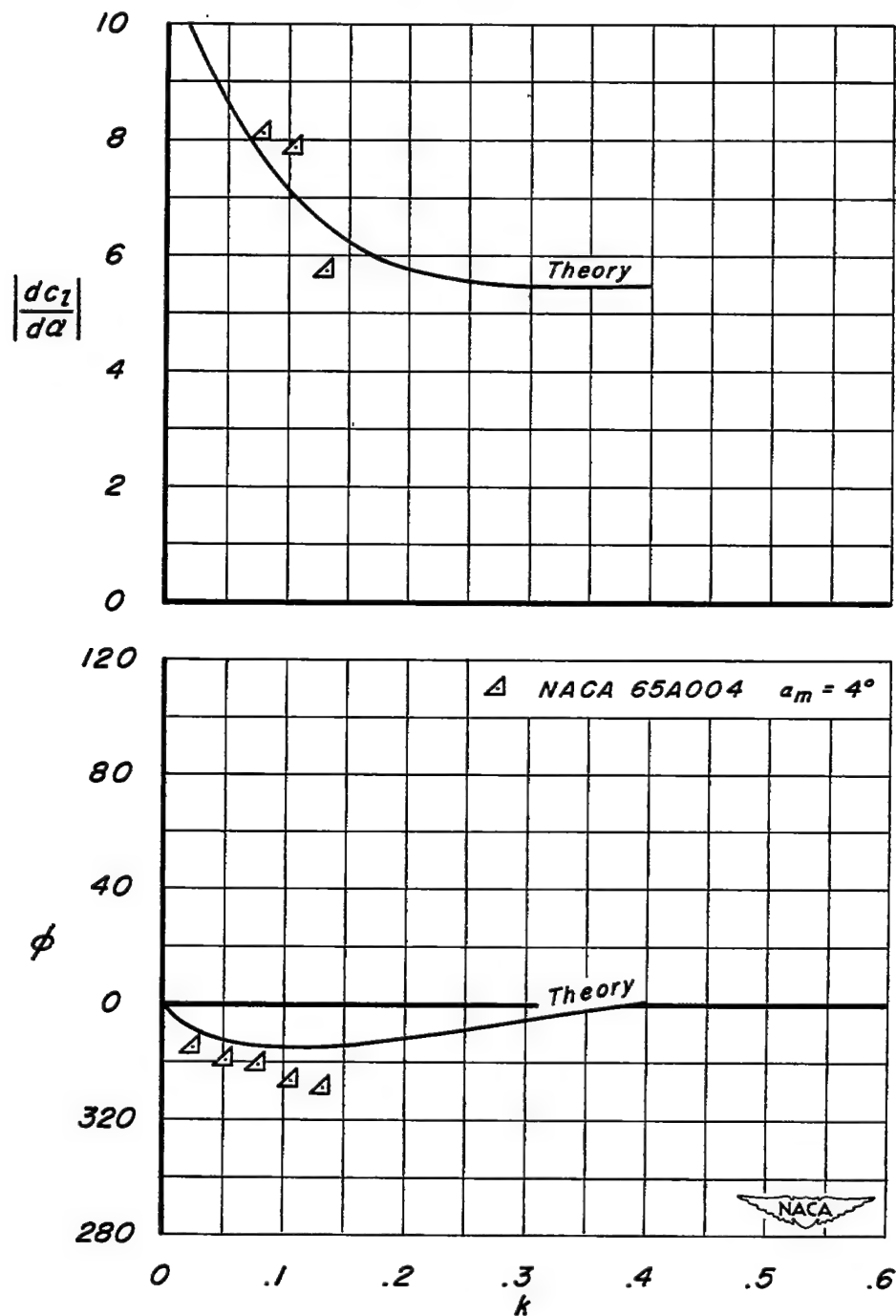
(f) Lift derivative and phase angle as a function of
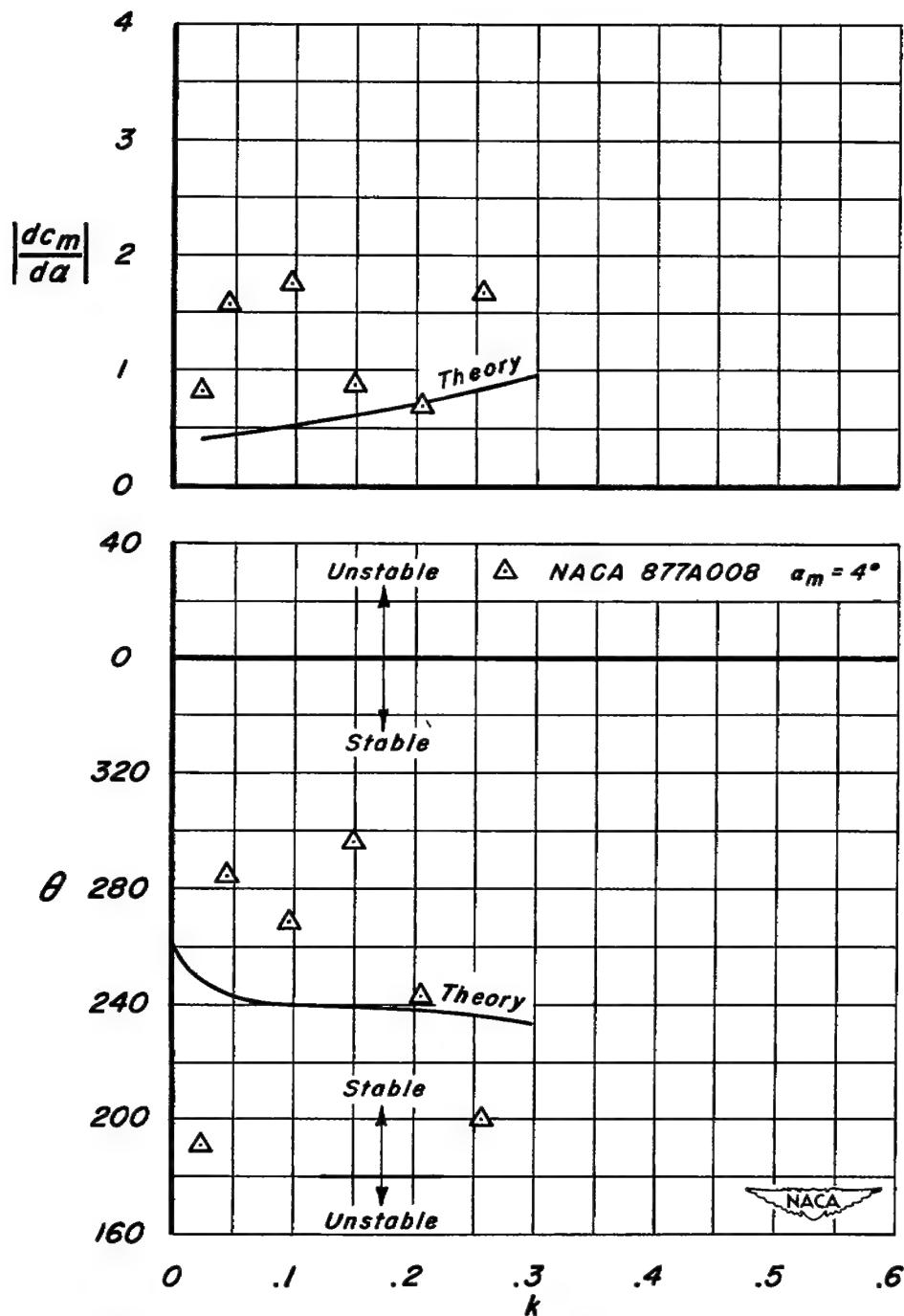reduced frequency. M = 0.83.
Figure 4.- Continued.
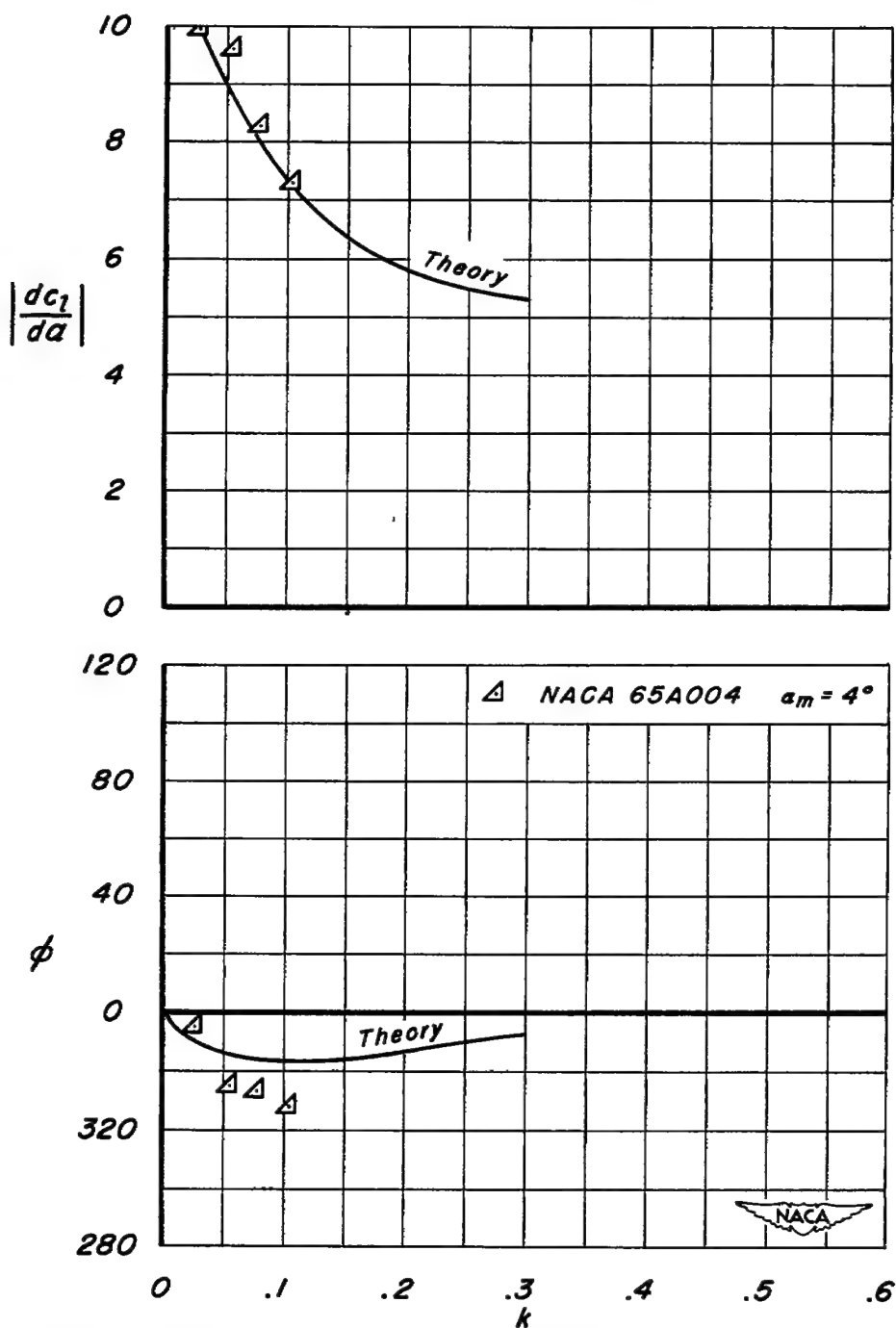
(g) Lift derivative and phase angle as a function of
reduced frequency. M = 0.87.

Figure 4.- Concluded.
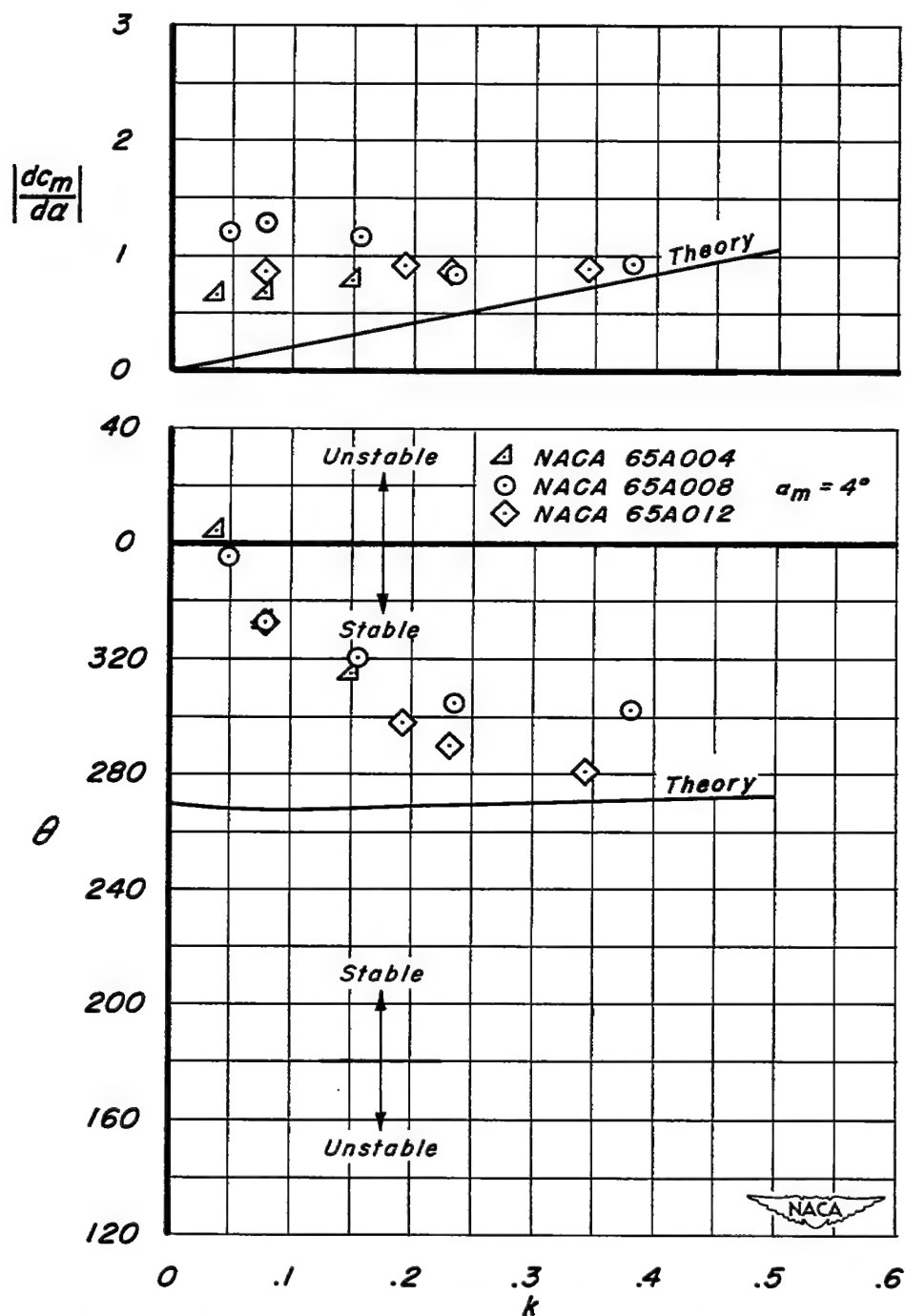
(a) Moment derivative and phase angle as a function of
reduced frequency. M = 0.59.

Figure 5.- Effects of airfoil thickness on moment flutter
derivative and phase angle.
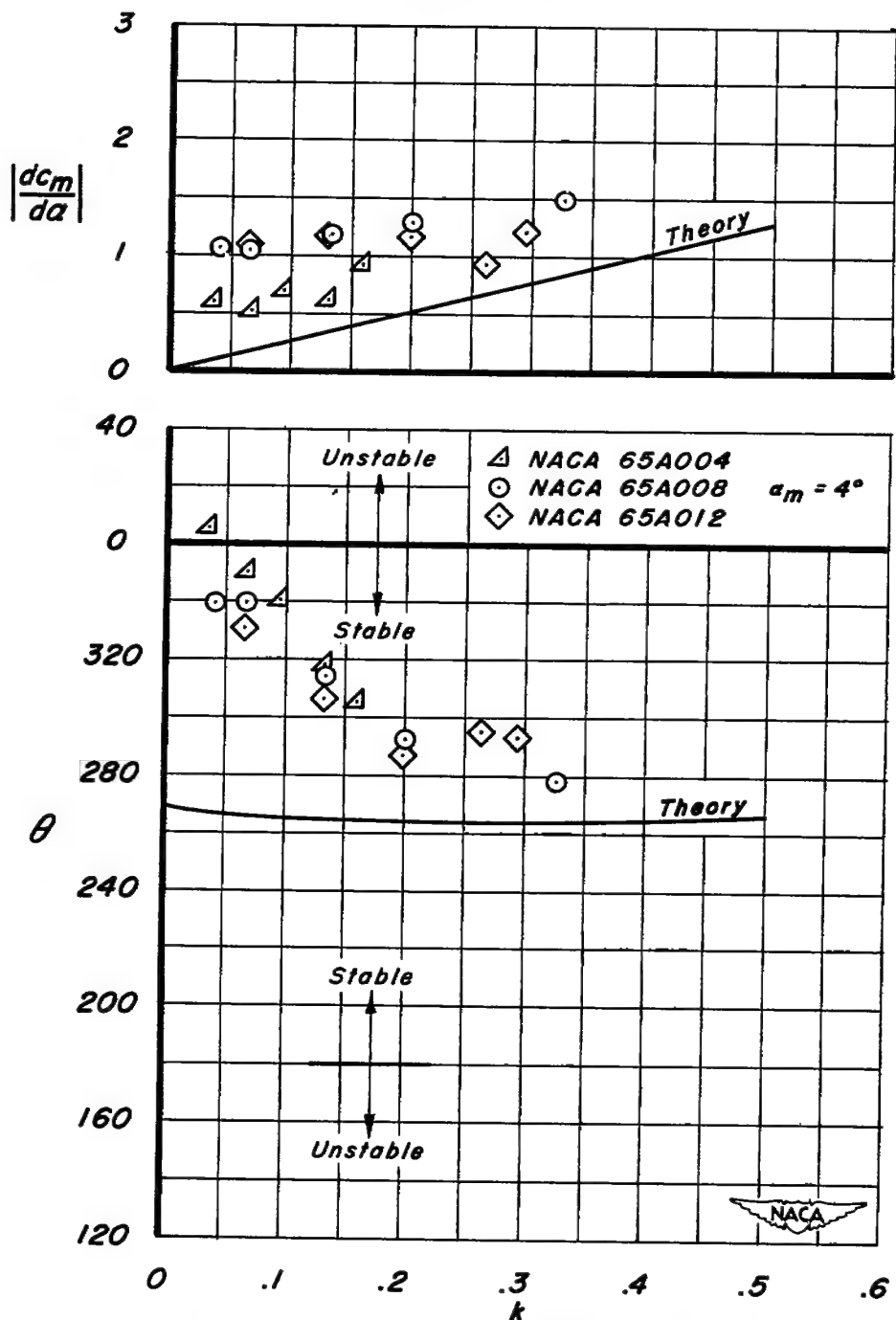
(b) Moment derivative and phase angle as a function of
reduced frequency. M = 0.68.

Figure 5.- Continued.

$\left|\dfrac{dc_m}{d\alpha}\right|$

Theory

Unstable

△ NACA 65A004
⊙ NACA 65A008 $a_m = 4°$
◇ NACA 65A012

Stable

Stable

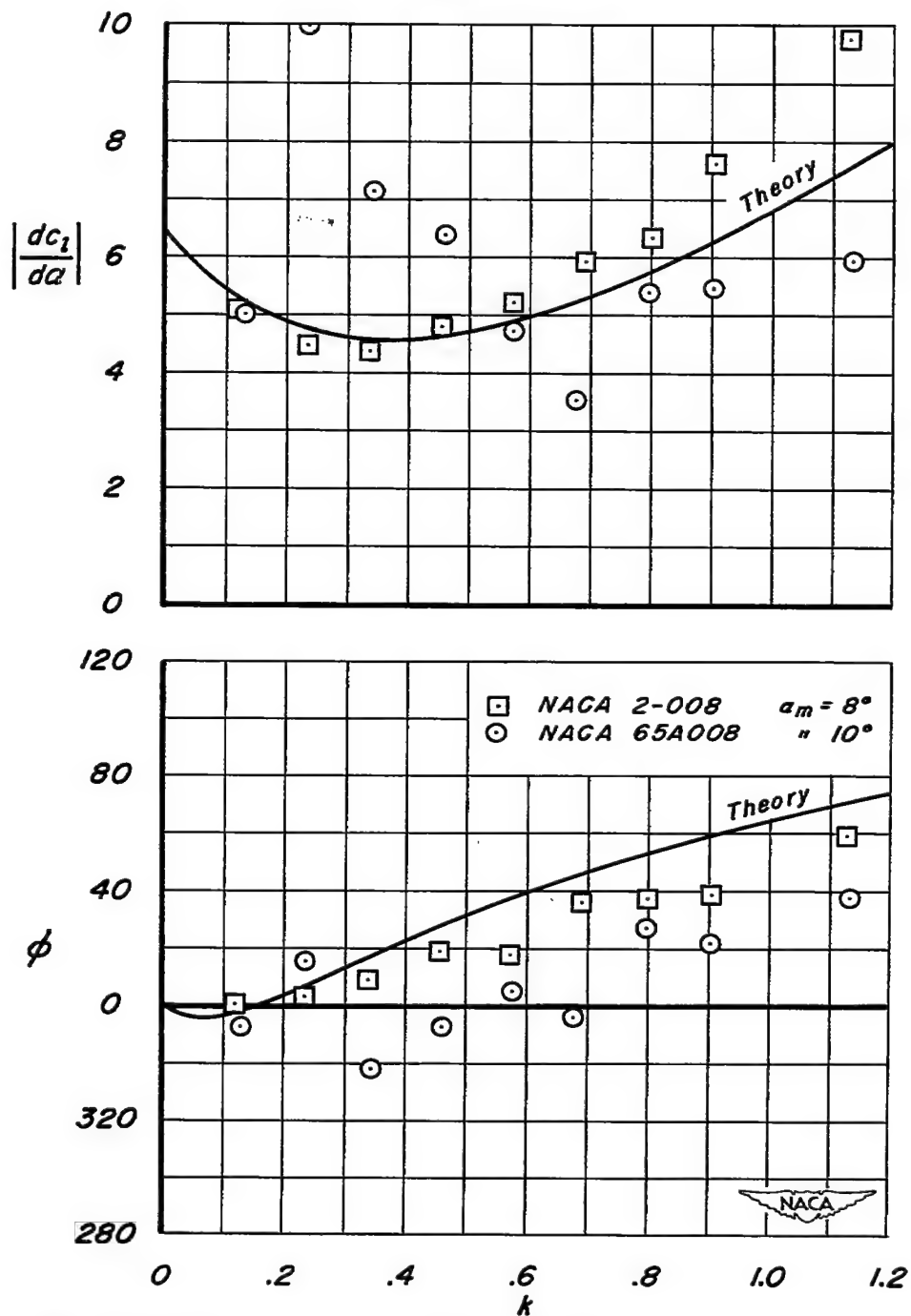Theory

Stable

Unstable

θ

k
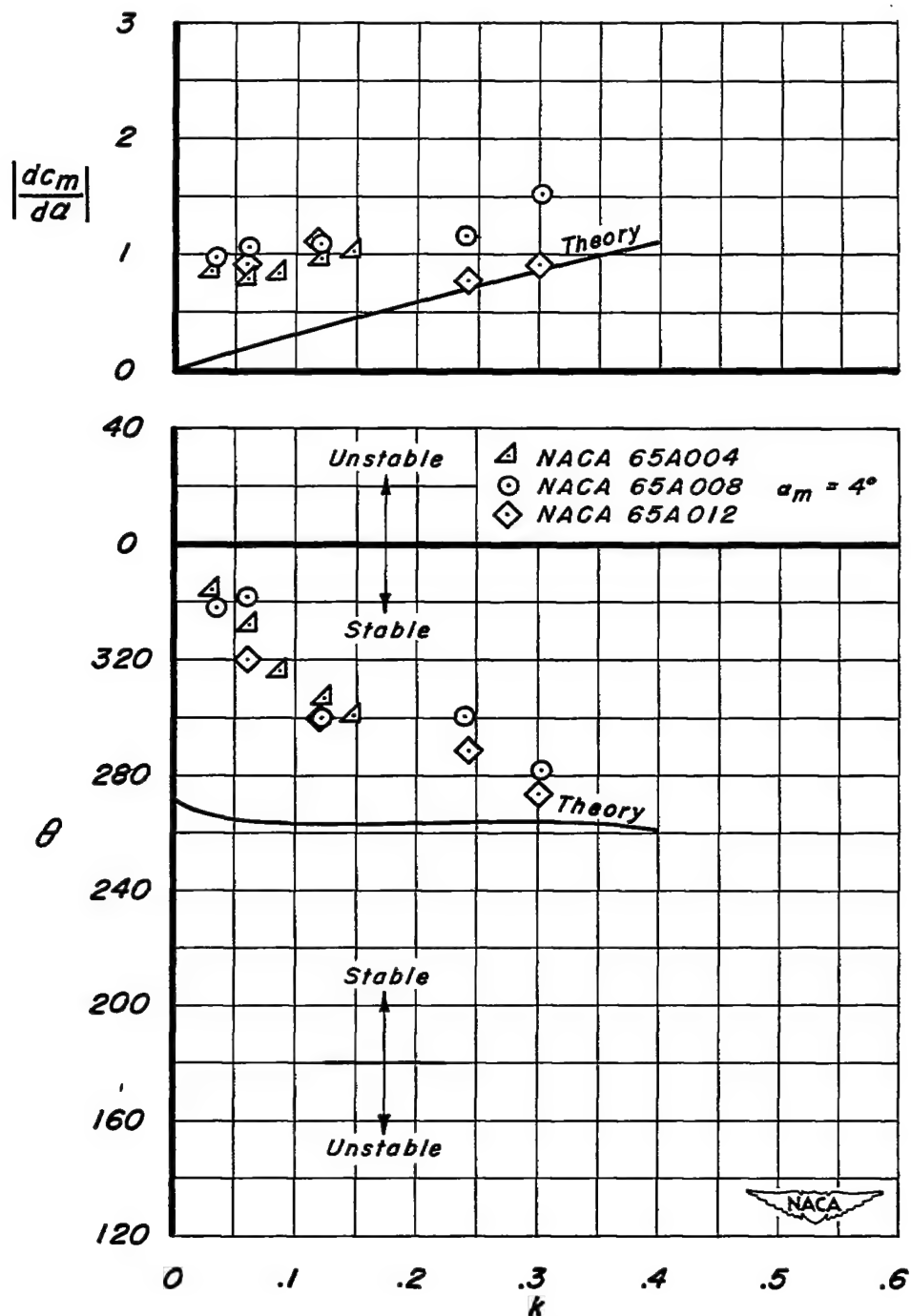
(c) Moment derivative and phase angle as a function of
reduced frequency. M = 0.73.

Figure 5.- Continued.
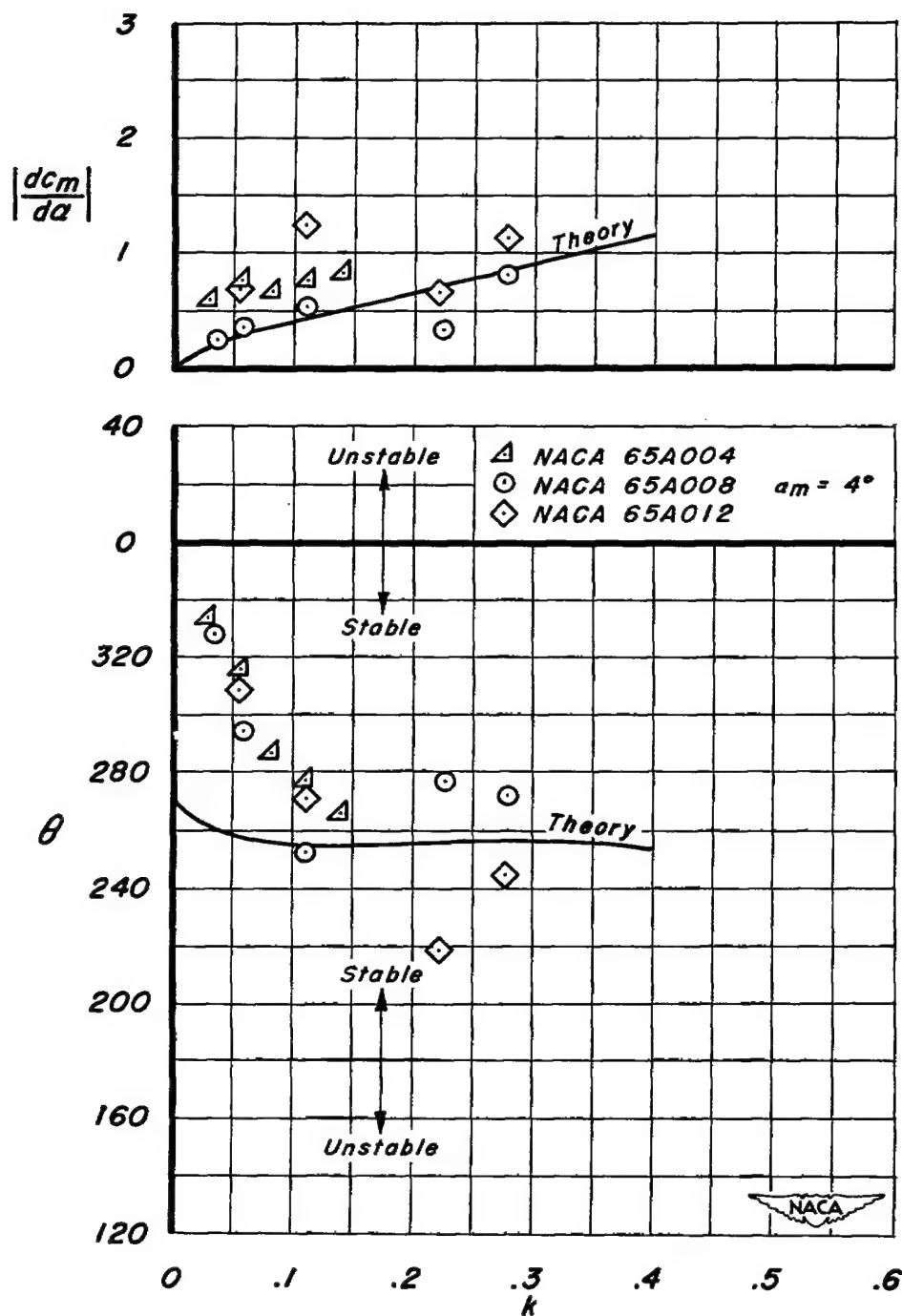
(d) Moment derivative and phase angle as a function of
reduced frequency. M = 0.79.

Figure 5.- Continued.
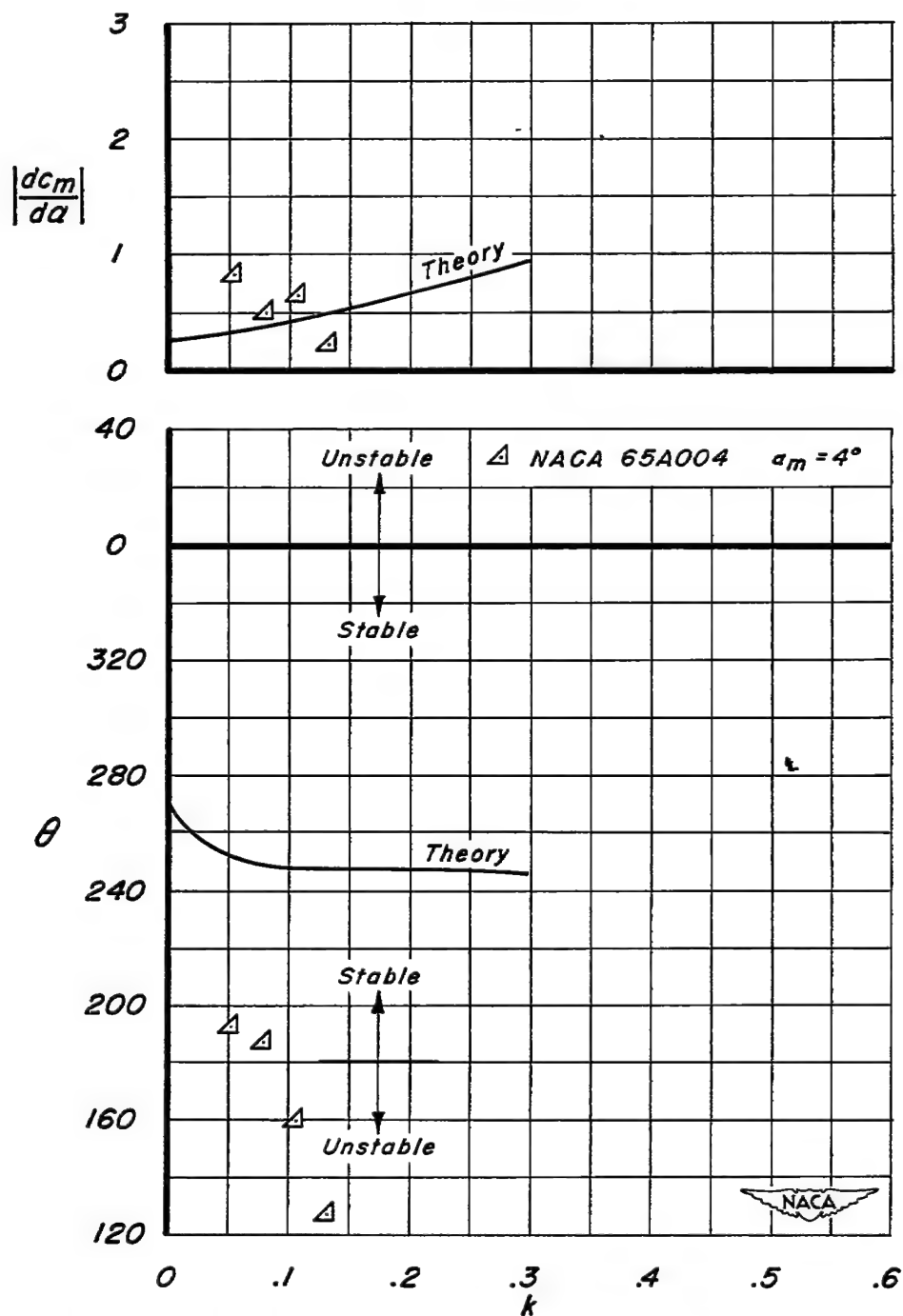
(e) Moment derivative and phase angle as a function of
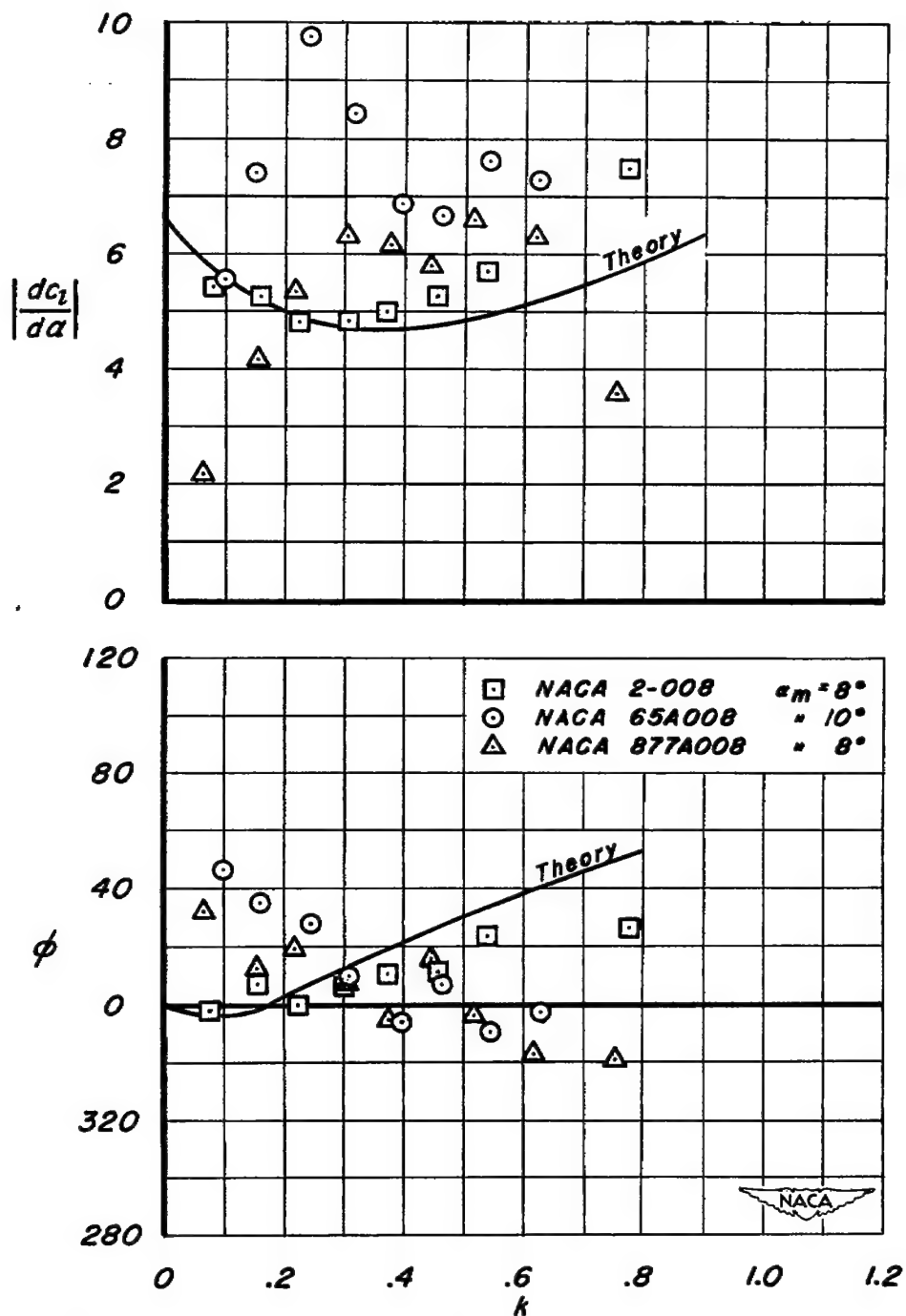reduced frequency. M = 0.83.

Figure 5.- Continued.
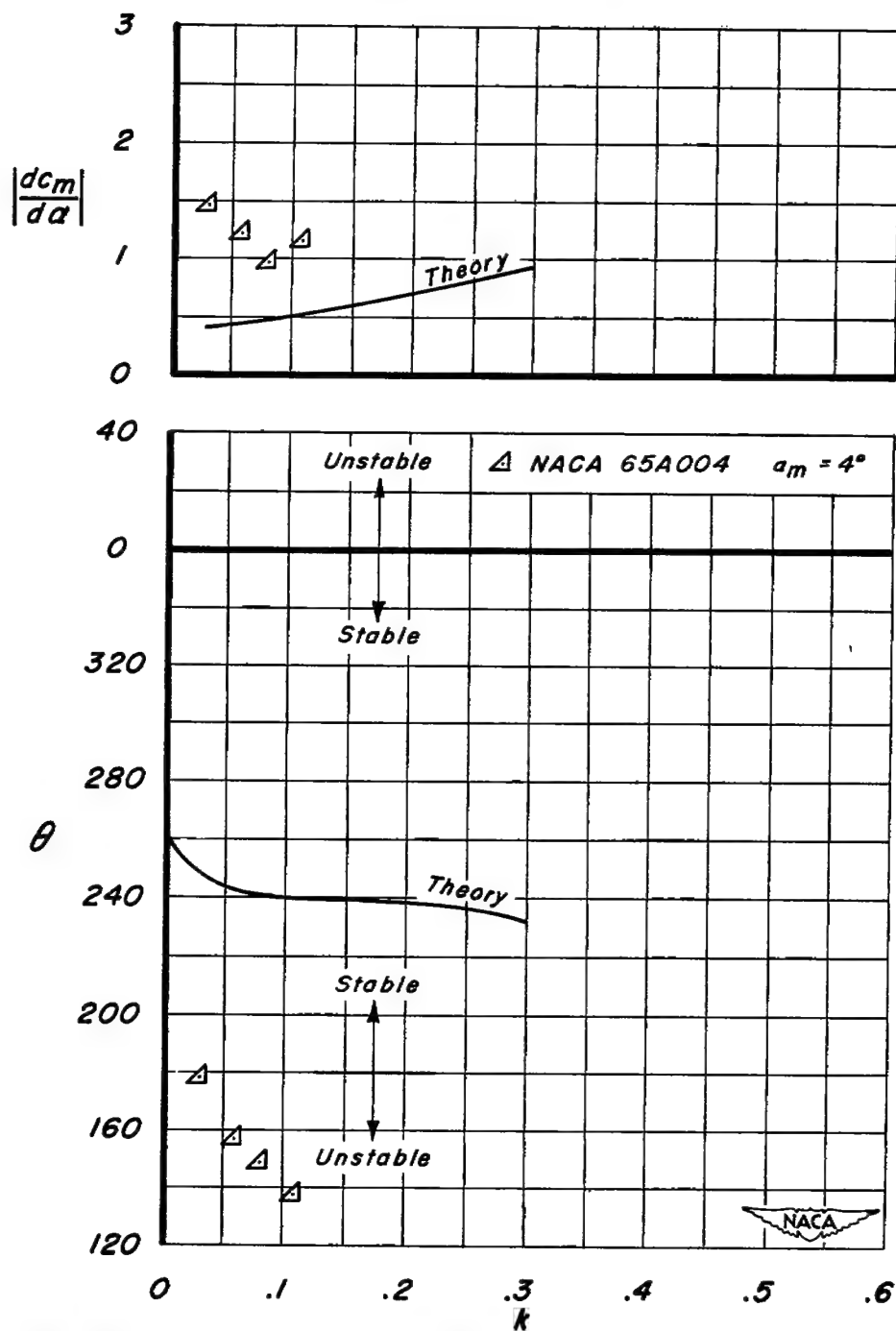
(f) Moment derivative and phase angle as a function of
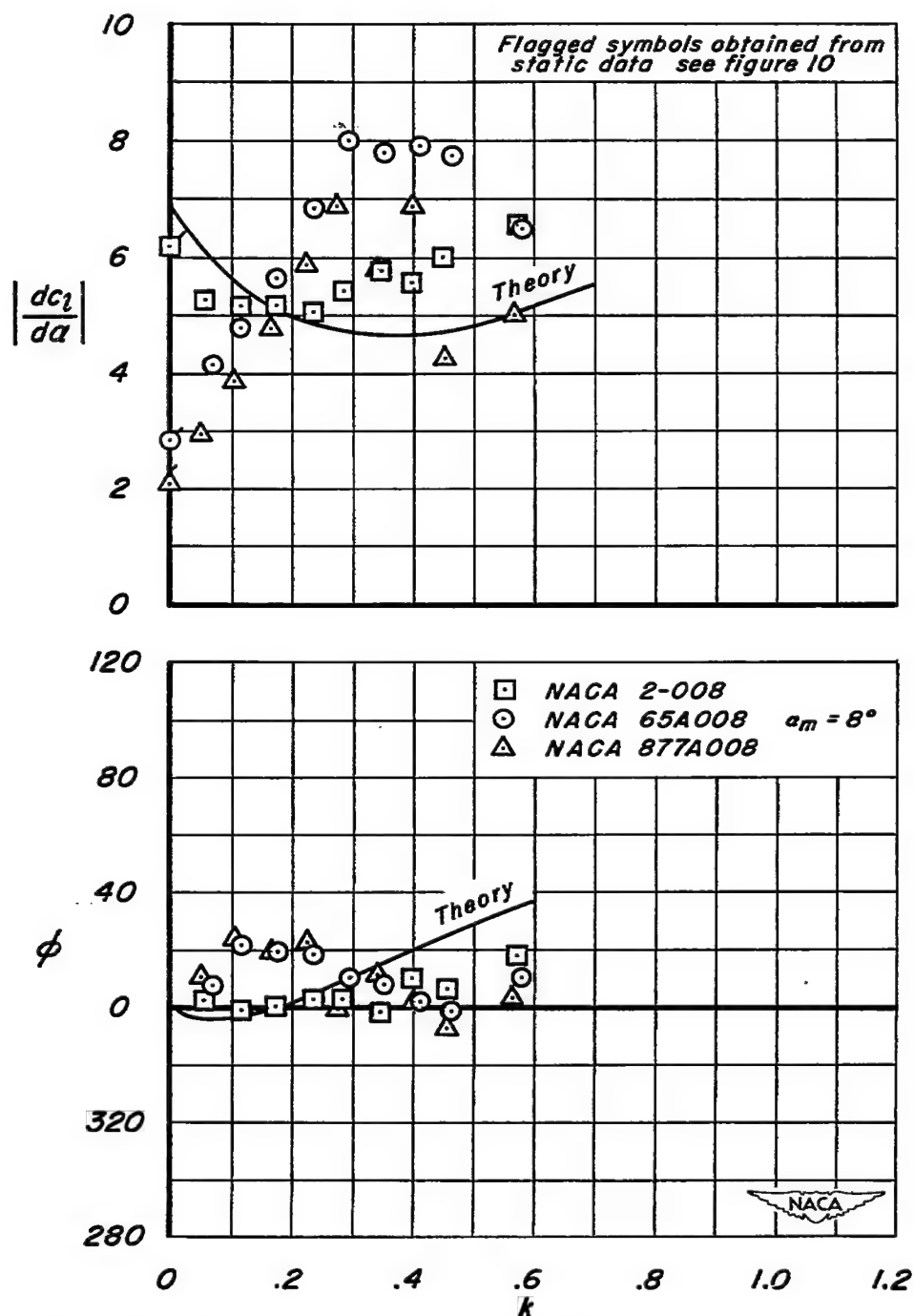reduced frequency. M = 0.87.

Figure 5.- Concluded.
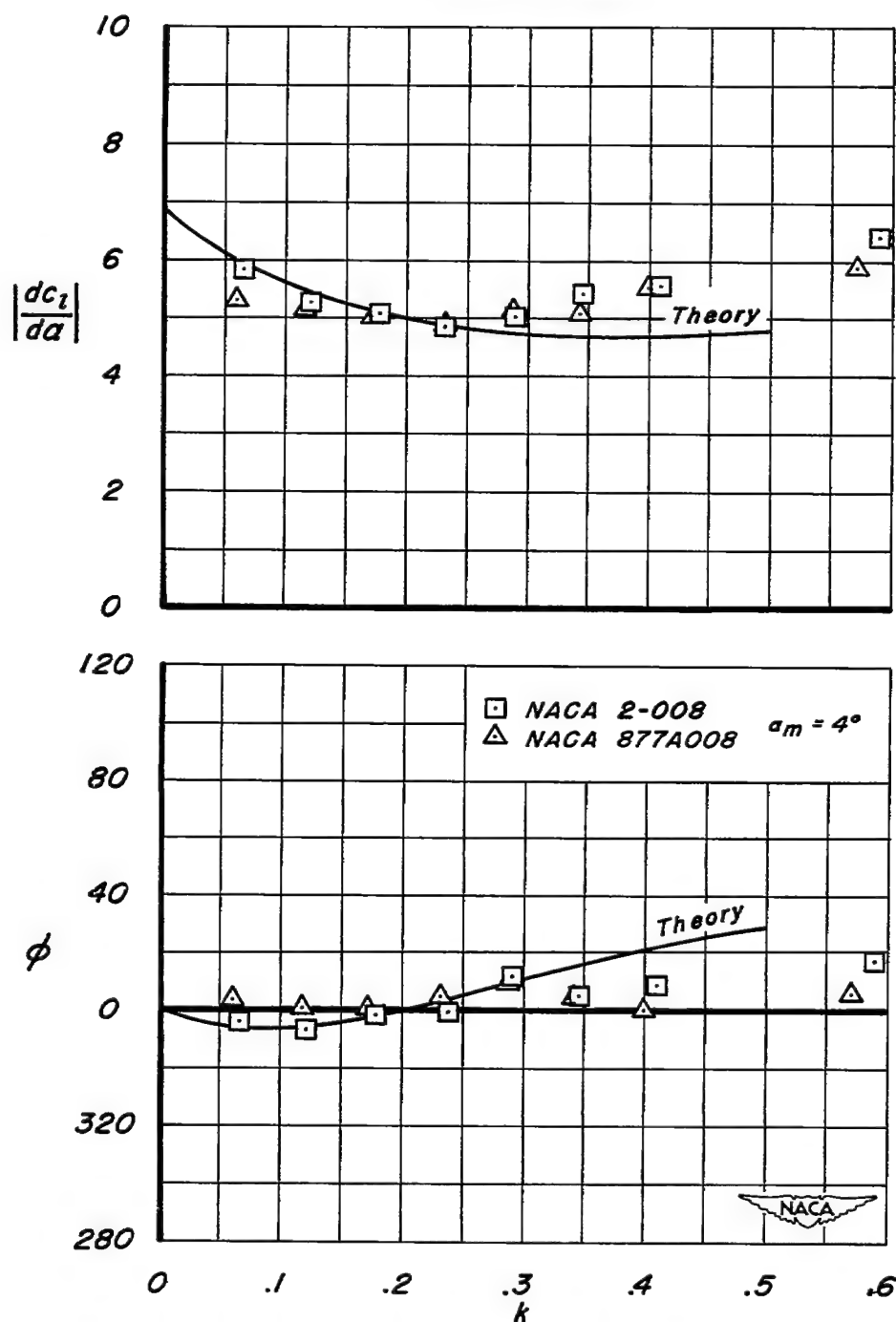
(a) Lift derivative and phase angle as a function of
reduced frequency. M = 0.40.

Figure 6.- Effects of airfoil thickness distribution on lift
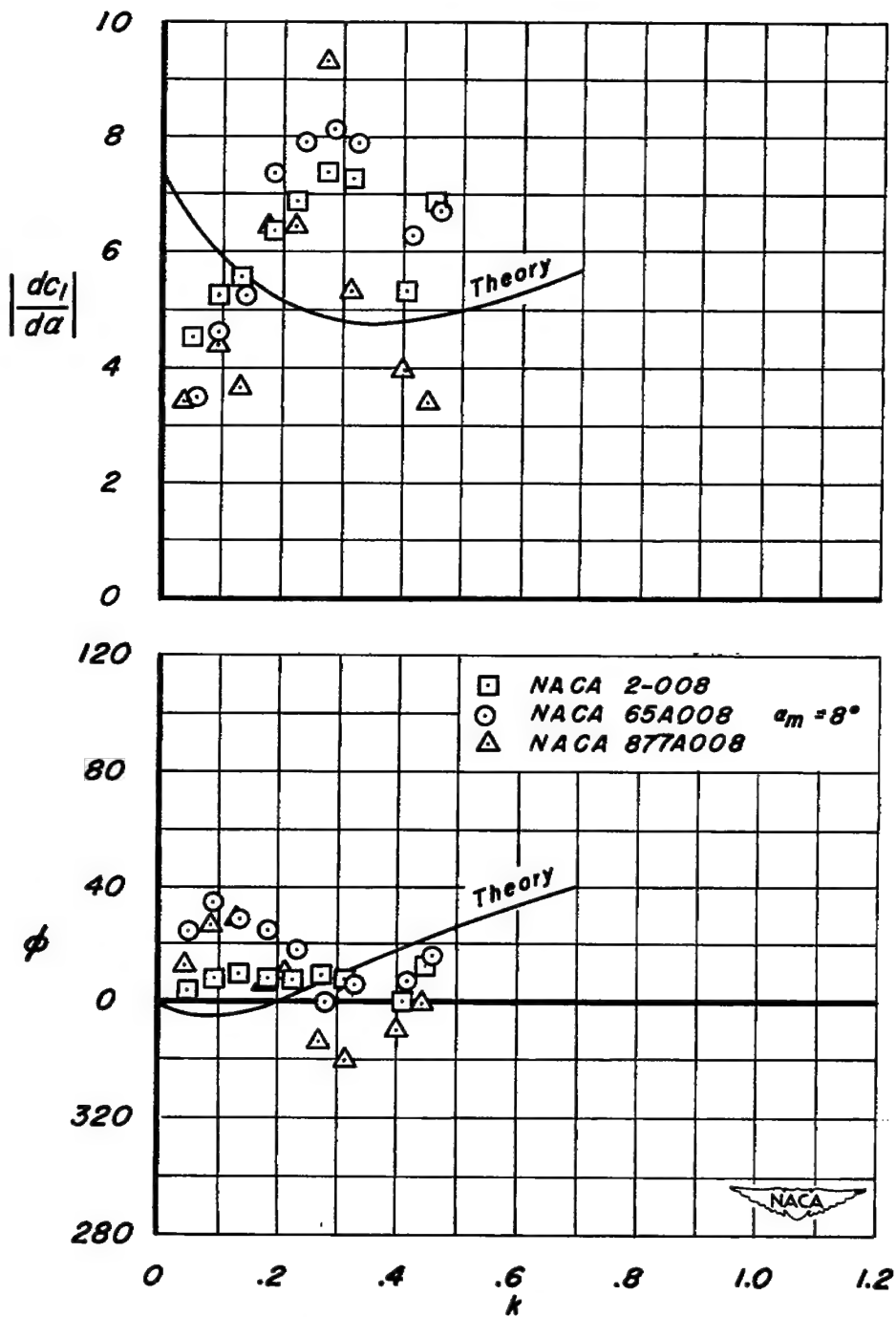flutter derivative and phase angle.

$\left|\dfrac{dc_l}{da}\right|$

Theory

ϕ

□ NACA 2-008
⊙ NACA 65A008 $a_m = 4°$
△ NACA 877A008

Theory

NACA
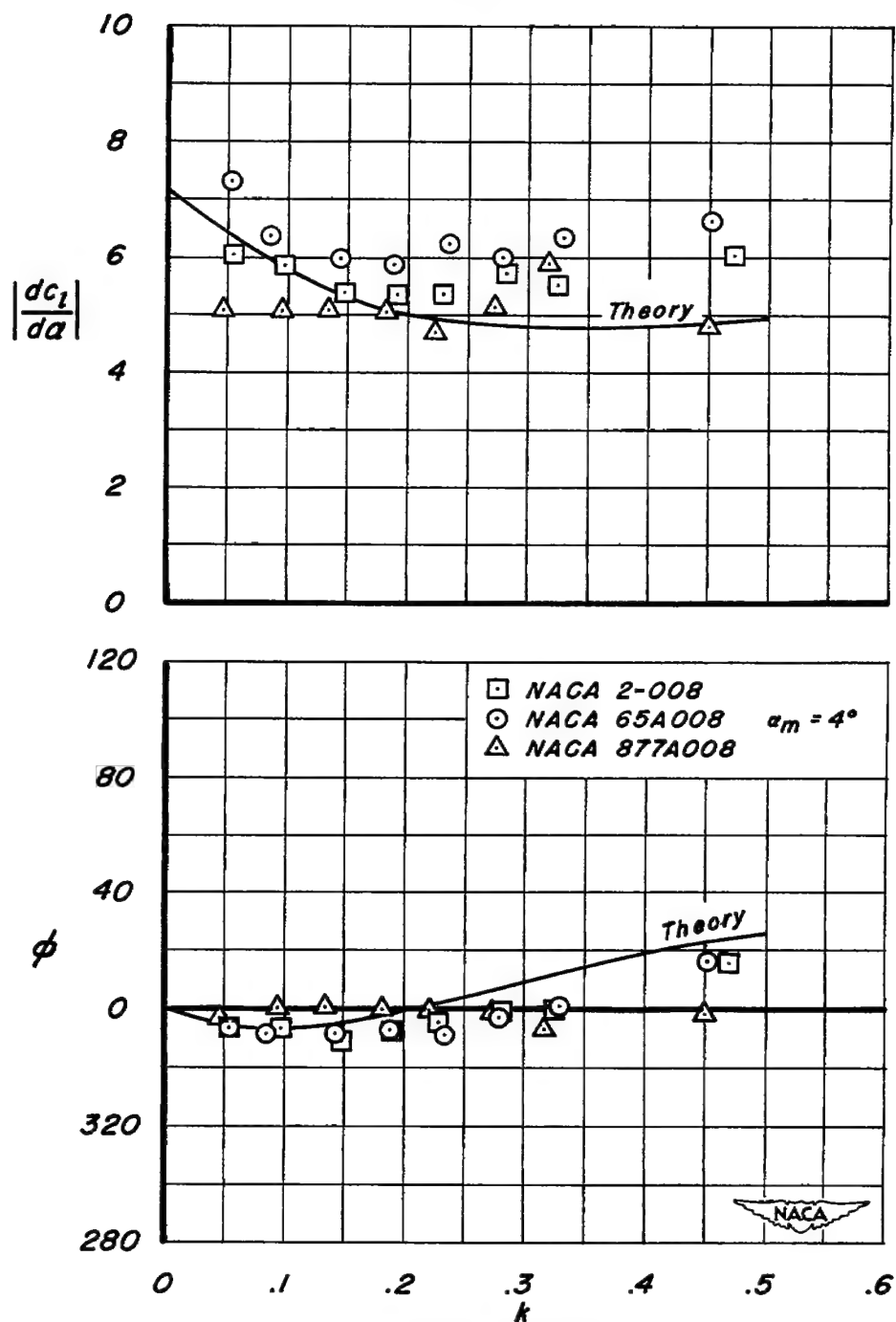
*(b) Lift derivative and phase angle a   a function of
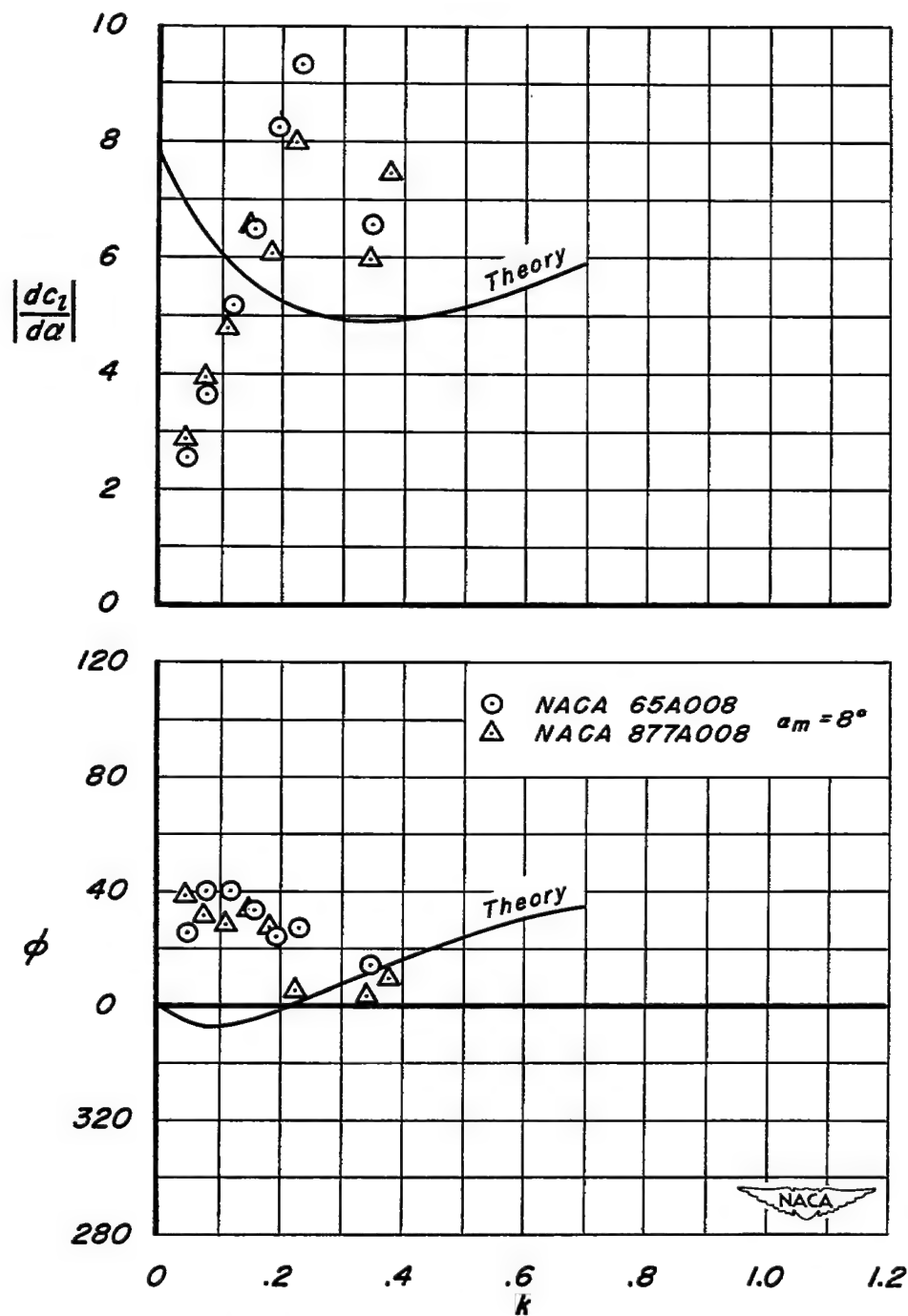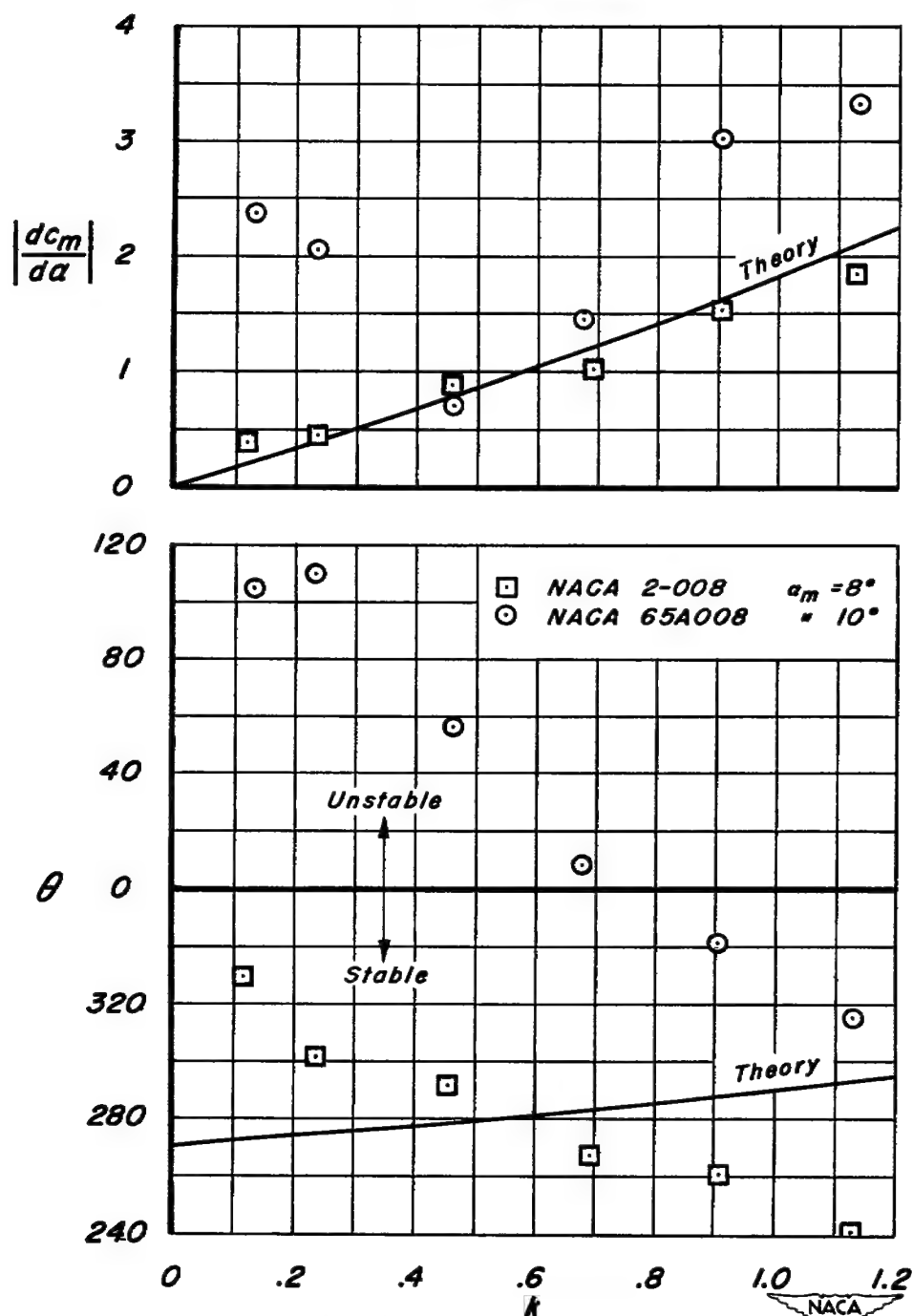reduced frequency. M = 0.49.*

Figure 6.- Continued.
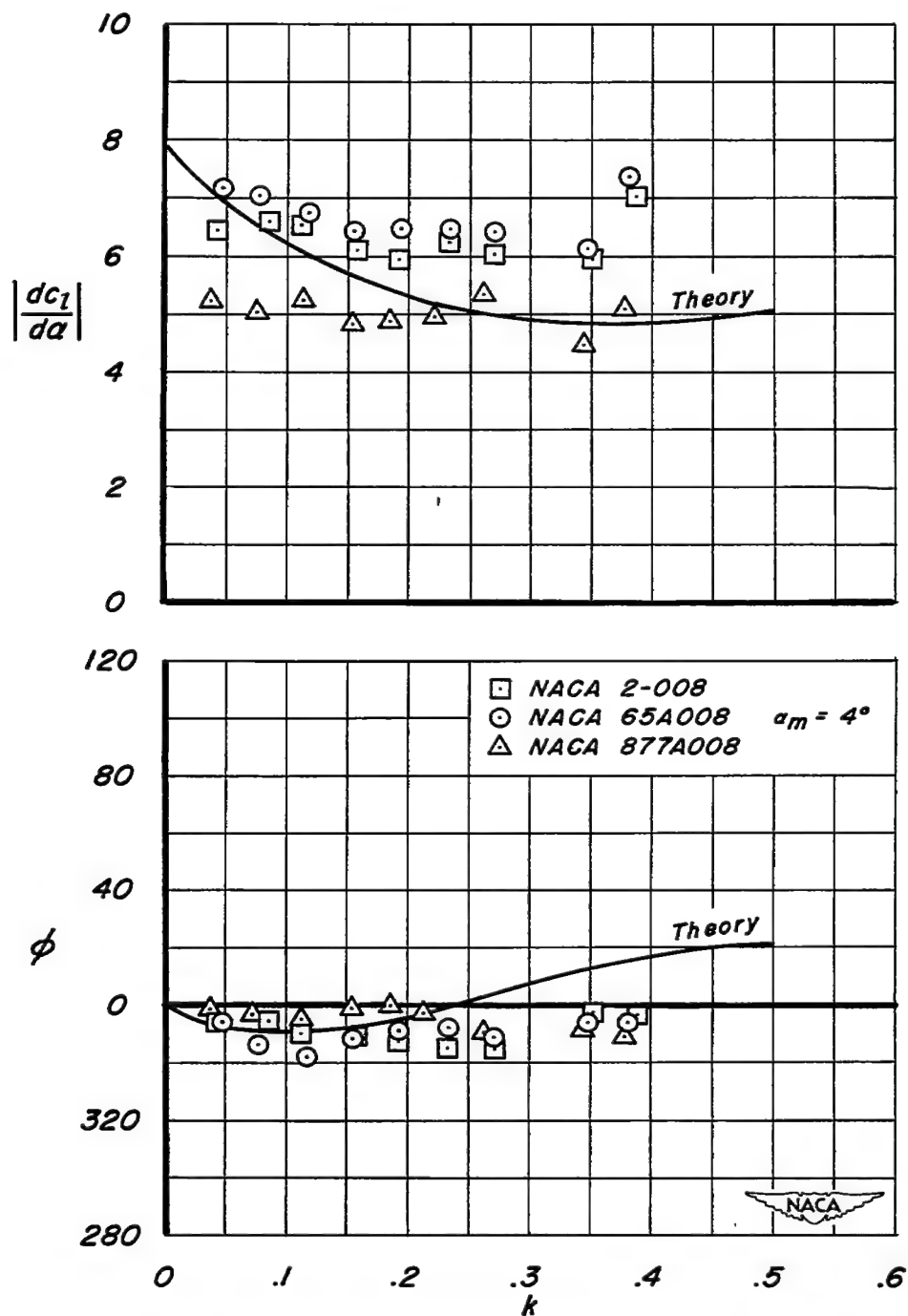
(c) Lift derivative and phase angle as a function of
reduced frequency. M = 0.59.

Figure 6.- Continued.
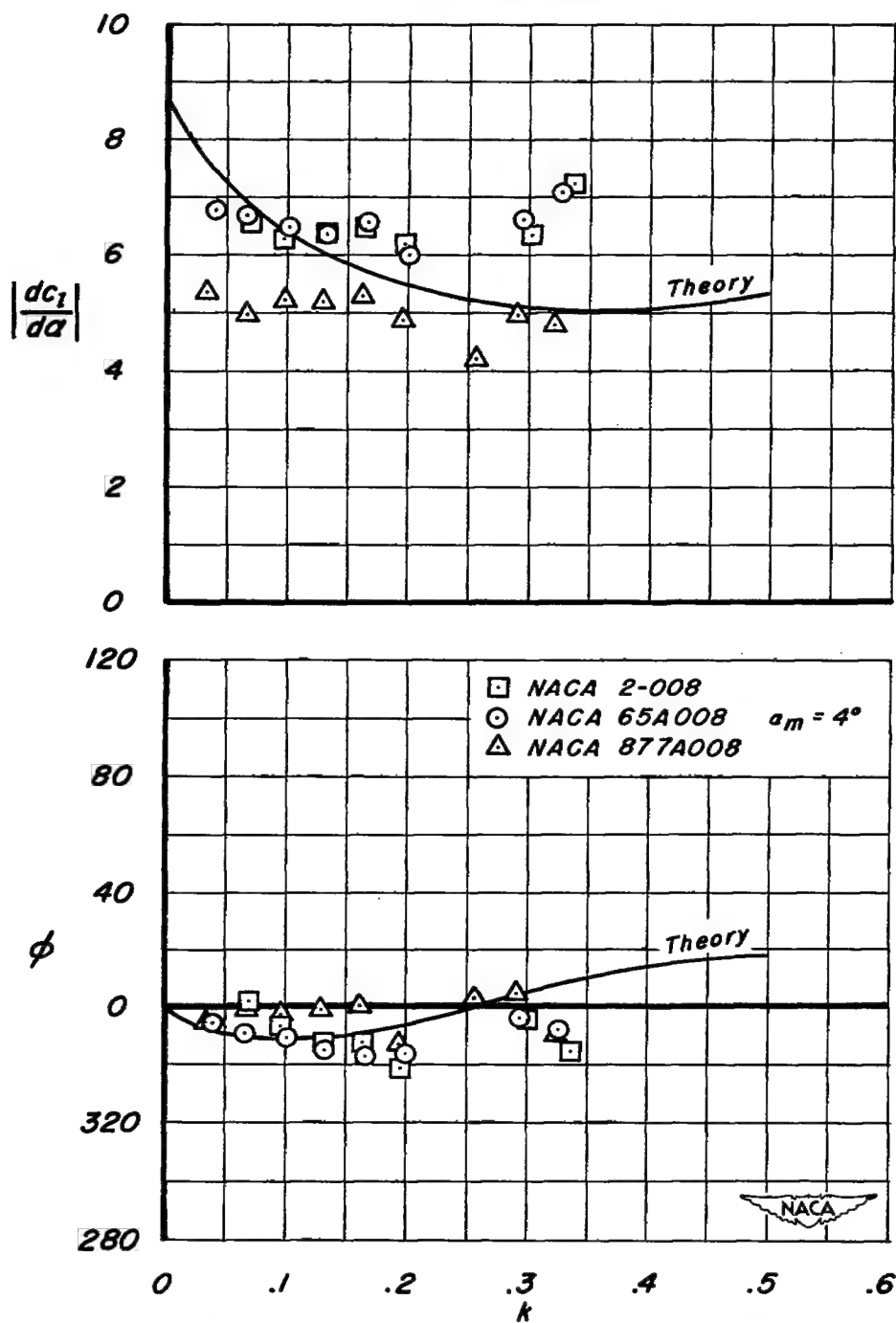
(d) Lift derivative and phase angle as a function of
reduced frequency. M = 0.68

Figure 6.- Continued.
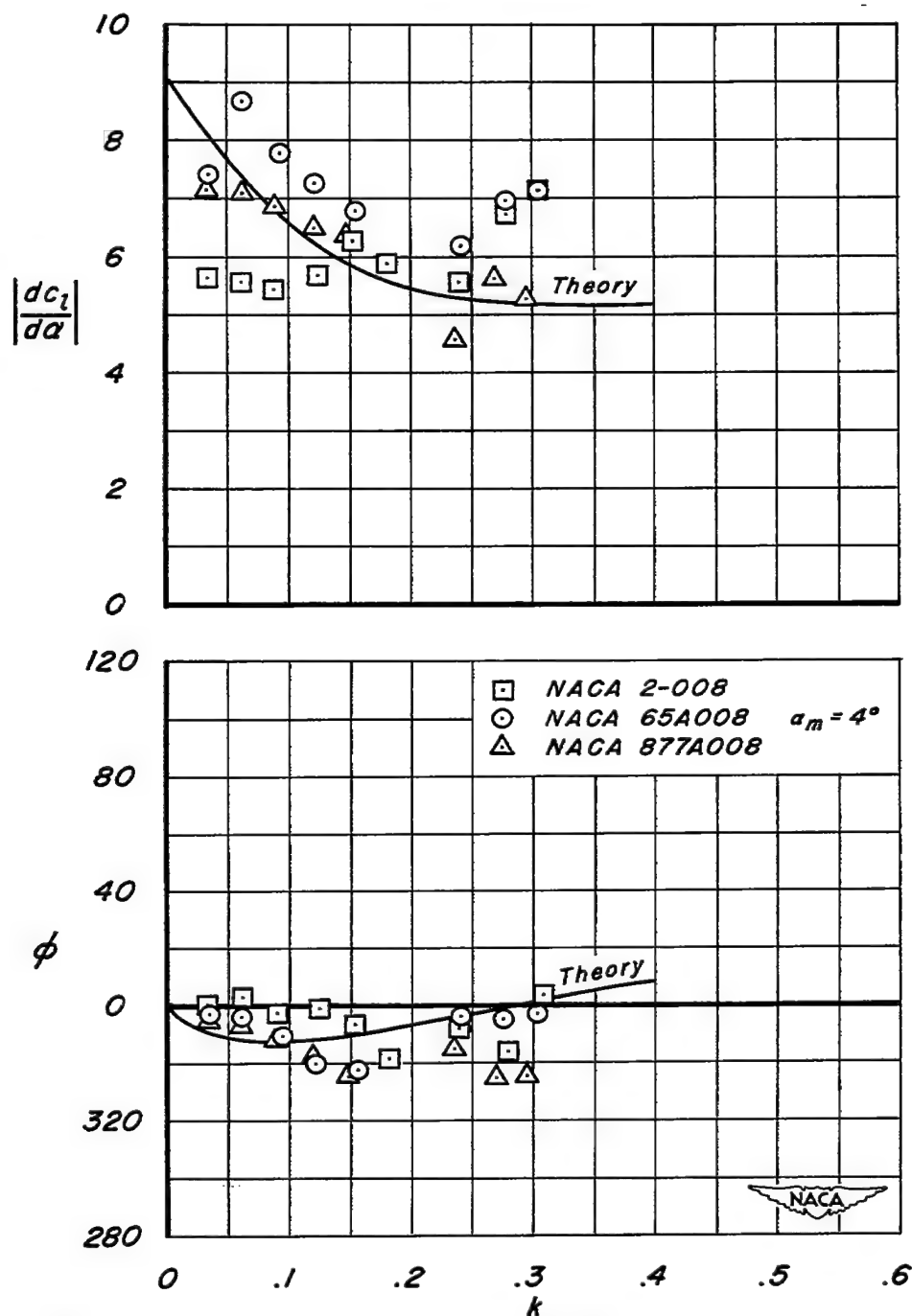
(e) Lift derivative and phase angle as a function of
reduced frequency. M = 0.73.
Figure 6.- Continued.
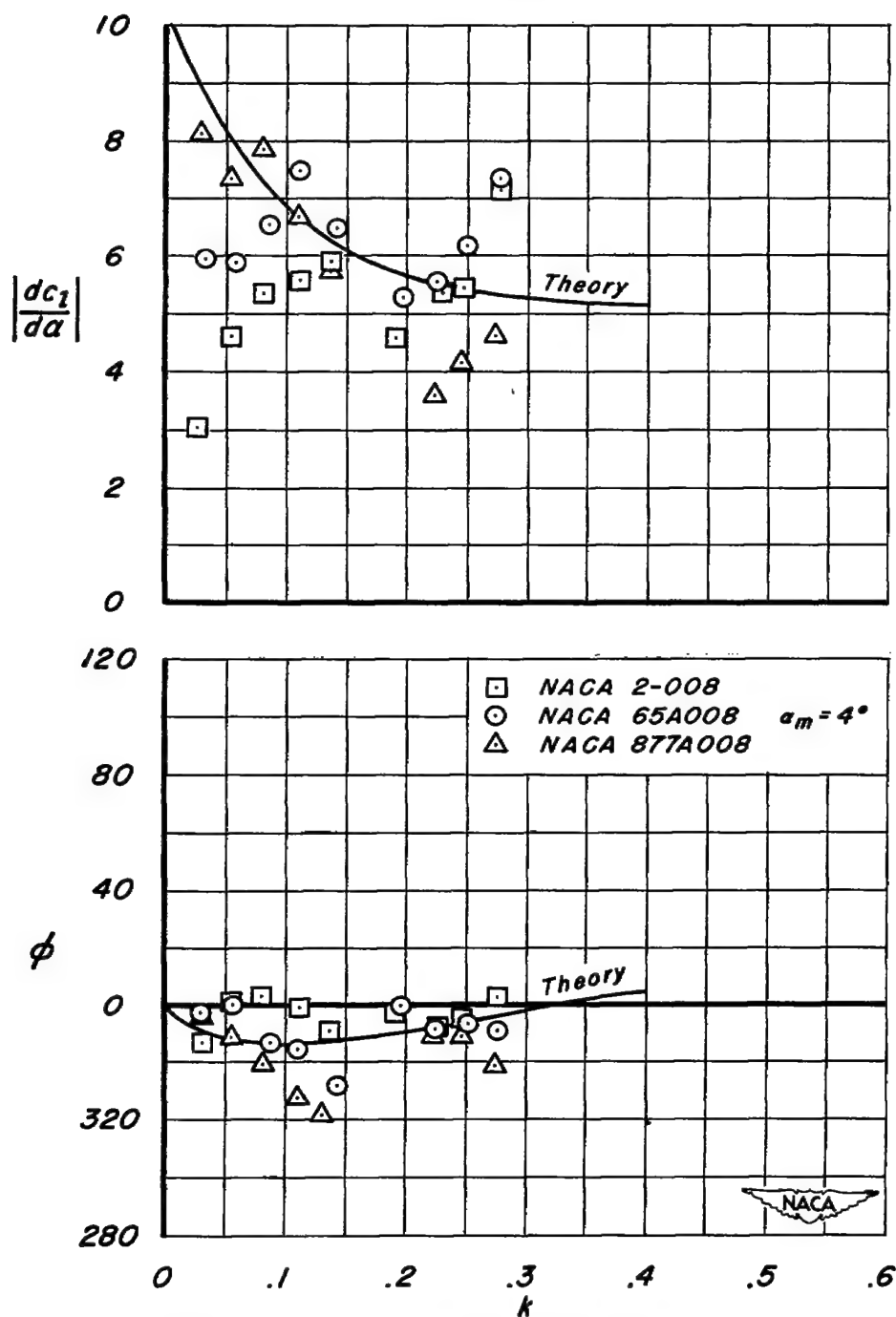
(f) Lift derivative and phase angle as a function of
reduced frequency. M = 0.79.
Figure 6.- Continued.
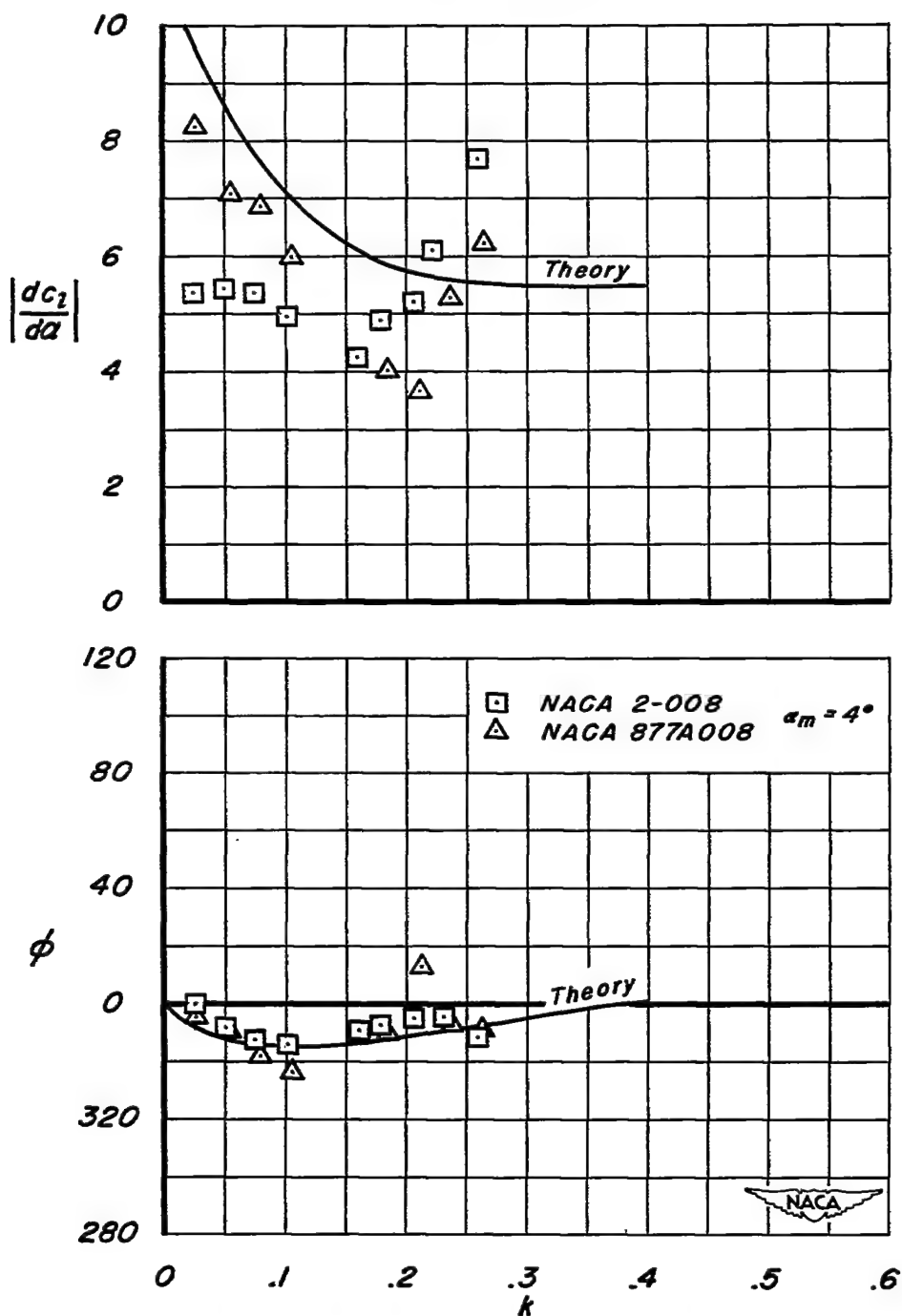
(g) Lift derivative and phase angle as a function of
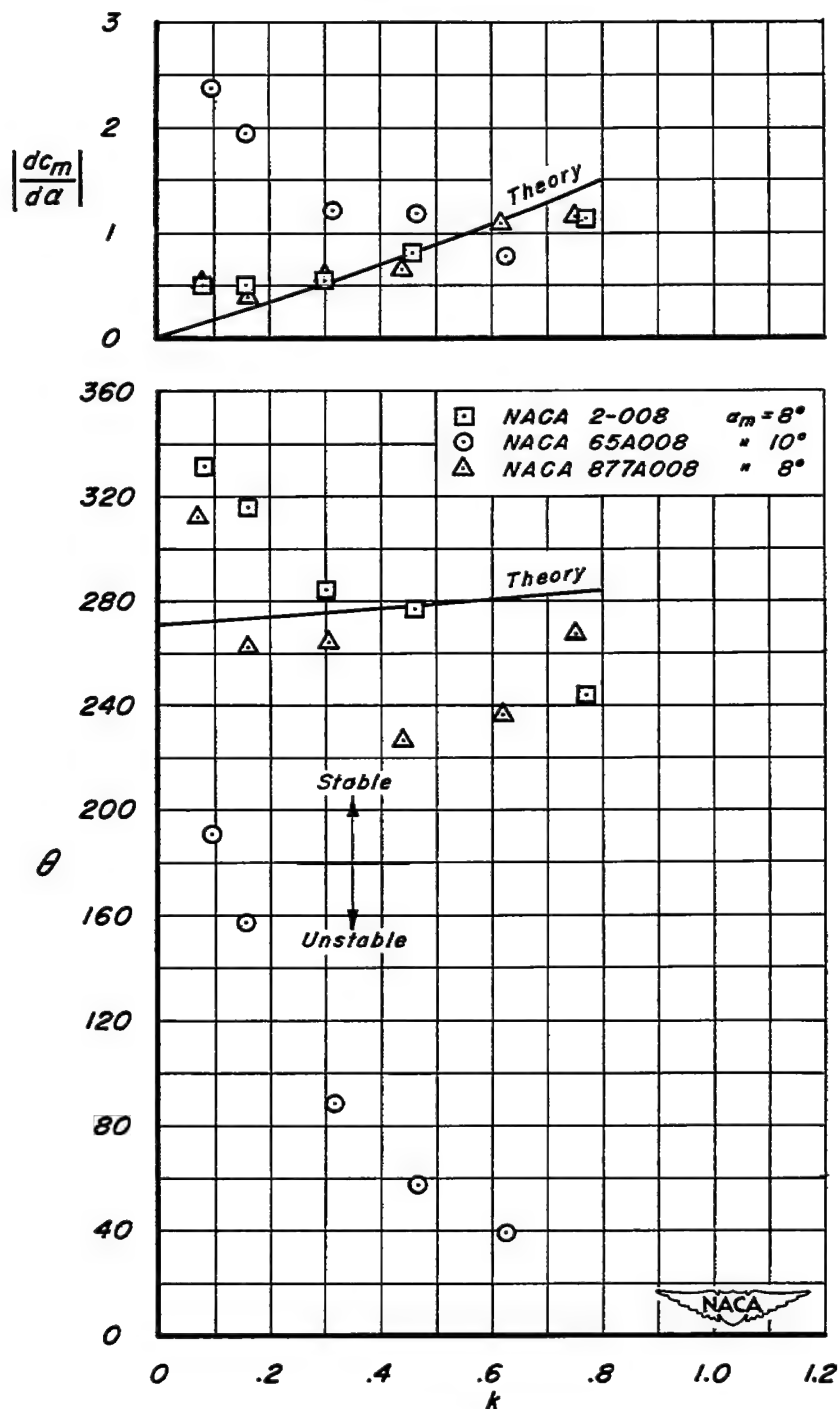reduced frequency. M = 0.83.

Figure 6.- Continued.
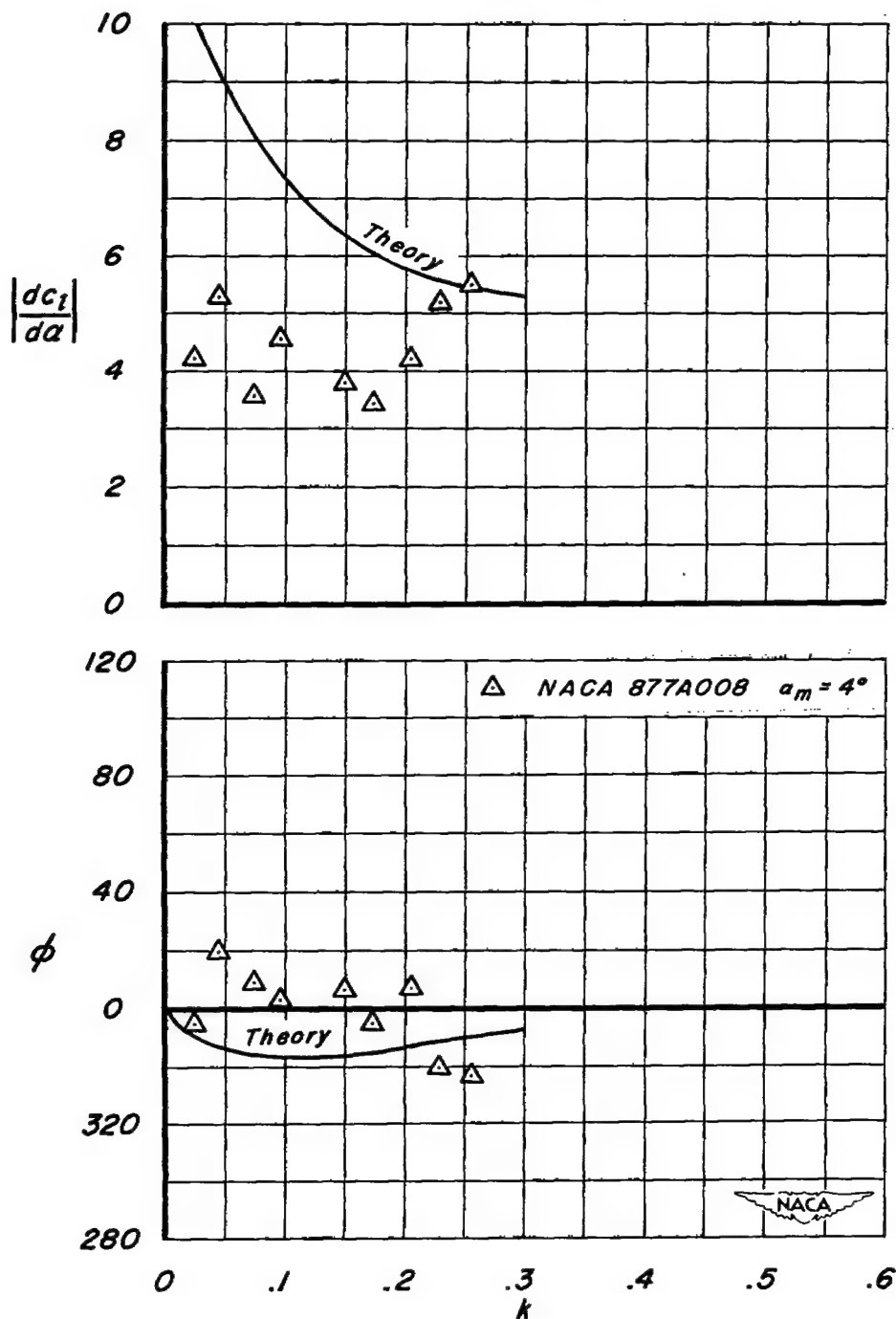
(h) Lift derivative and phase angle as a function of
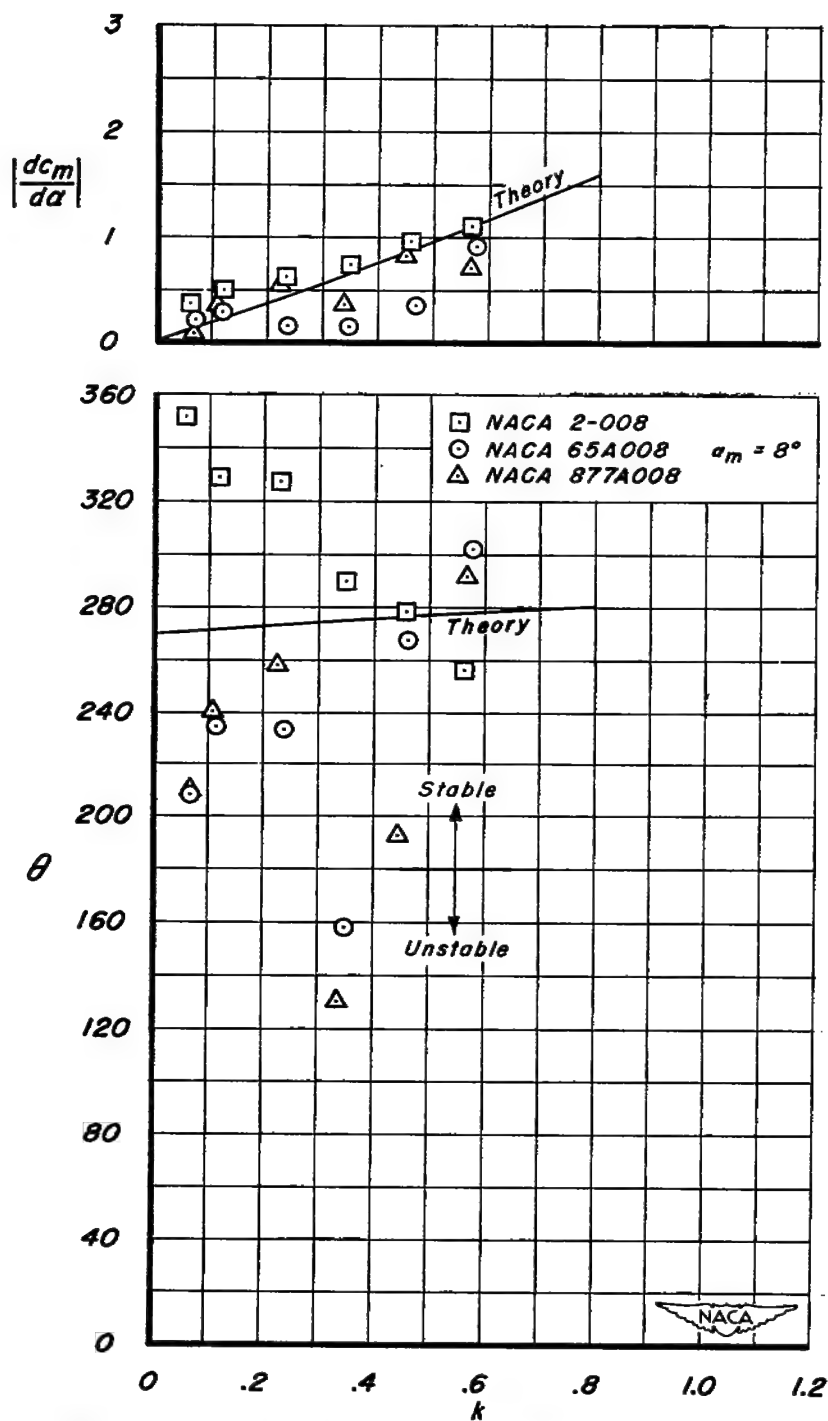reduced frequency. M = 0.86.

Figure 6.- Concluded.
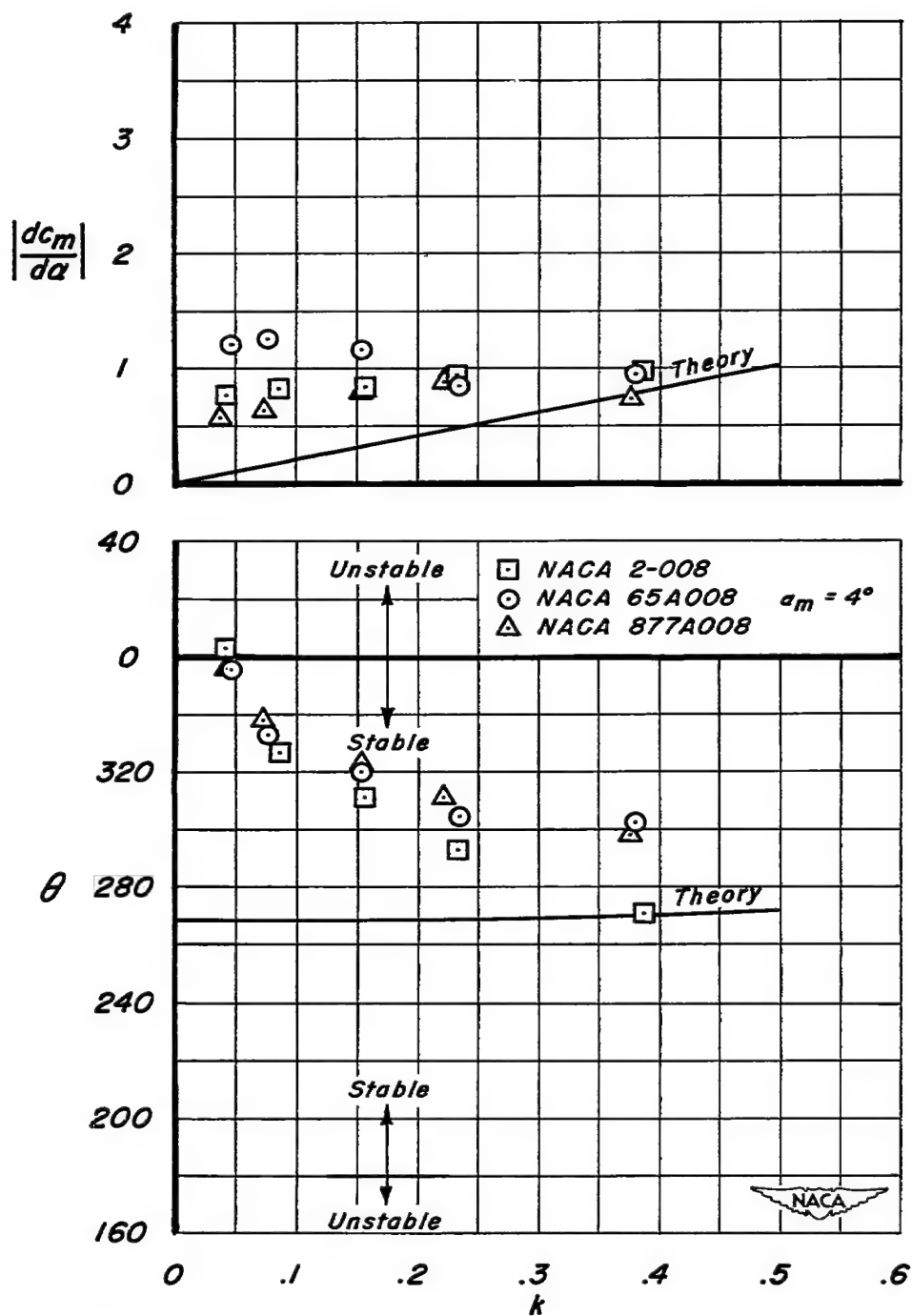
(a) Moment derivative and phase angle as a function of
reduced frequency. M = 0.59.

Figure 7.- Effects of airfoil thickness distribution on moment
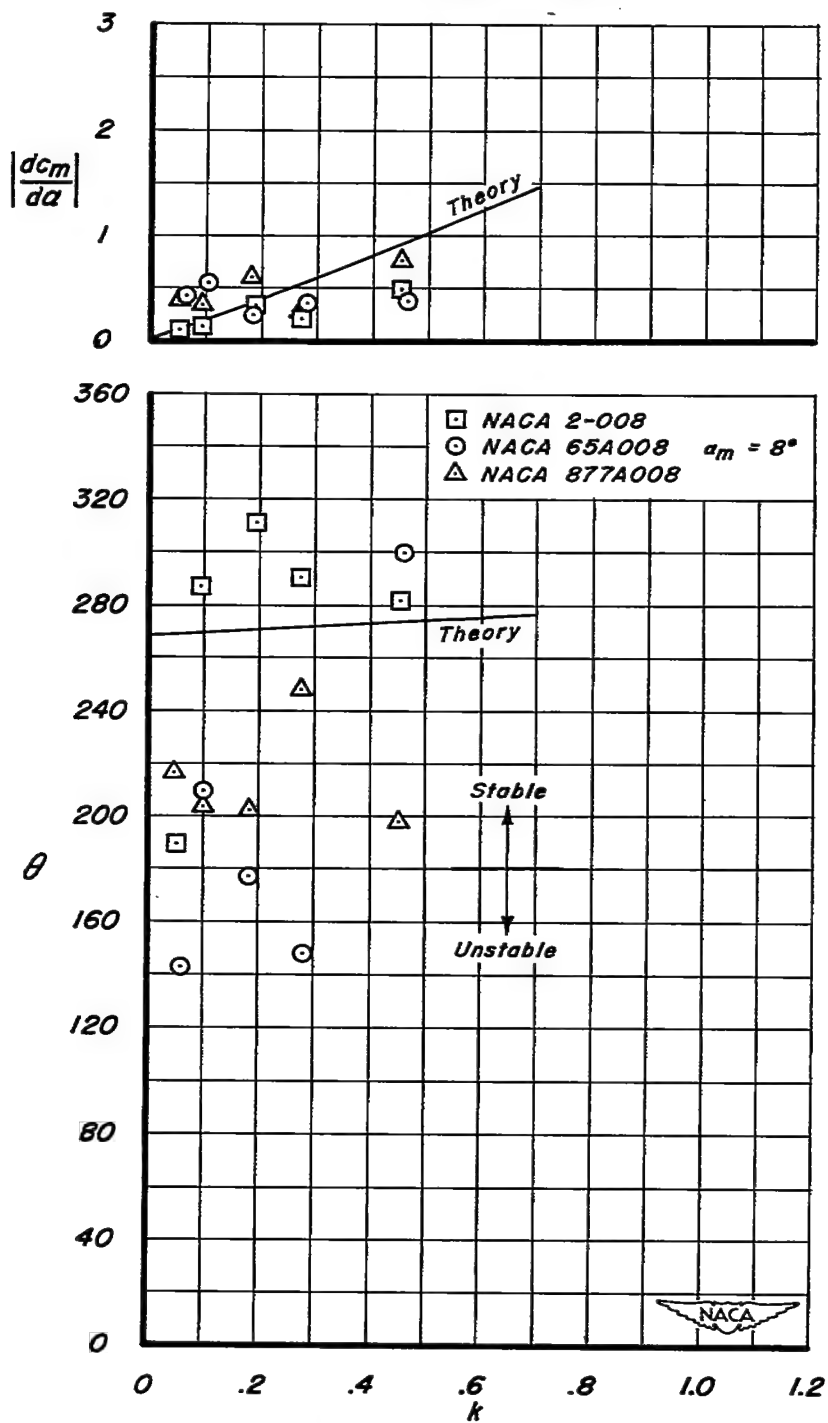flutter derivative and phase angle.

(b) Moment derivative and phase angle as a function of
reduced frequency. M = 0.68.

Figure 7.- Continued.

(c) Moment derivative and phase angle as a function of
reduced frequency. M = 0.73

Figure 7.- Continued.

(d) Moment derivative and phase angle as a function of
reduced frequency. M = 0.79.

Figure 7.- Continued.
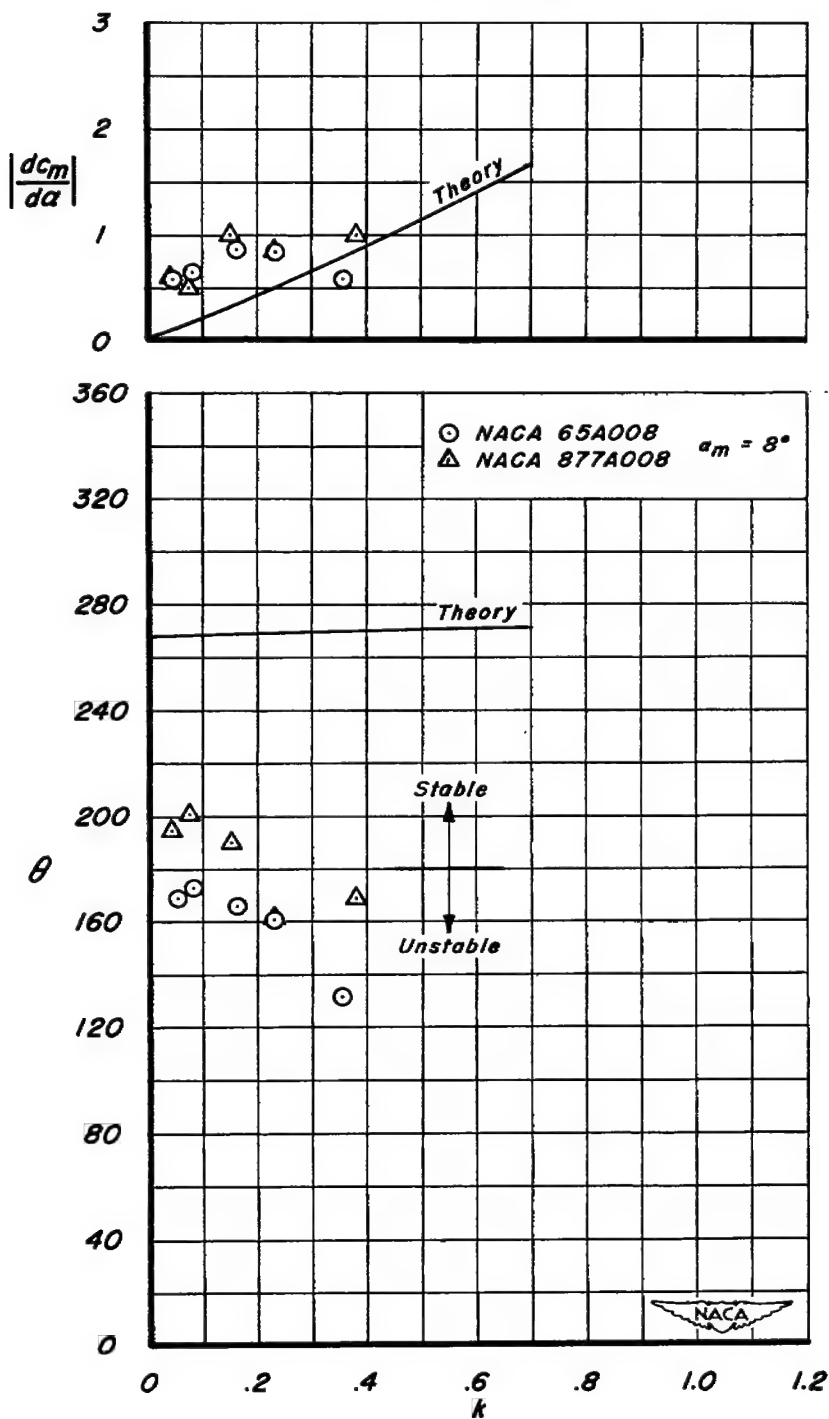
(e) Moment derivative and phase angle as a function of
reduced frequency. M = 0.83.
Figure 7.- Continued.

(f) Moment derivative and phase angle as a function of reduced frequency. M = 0.86.

Figure 7.- Concluded.

(a) Lift derivative and phase angle as a function of
reduced frequency. M = 0.20.

Figure 8.- Effects of airfoil thickness distribution on lift
flutter derivative and phase angle.

(b) Lift derivative and phase angle as a function of
reduced frequency. M = 0.30.

Figure 8.- Continued.

(c) Lift derivative and phase angle as a function of
reduced frequency. M = 0.40.

Figure 8.- Continued.

(d) Lift derivative and phase angle as a function of
reduced frequency. M = 0.50.

Figure 8.- Continued.

(e) Lift derivative and phase angle as a function of reduced frequency. M = 0.59.
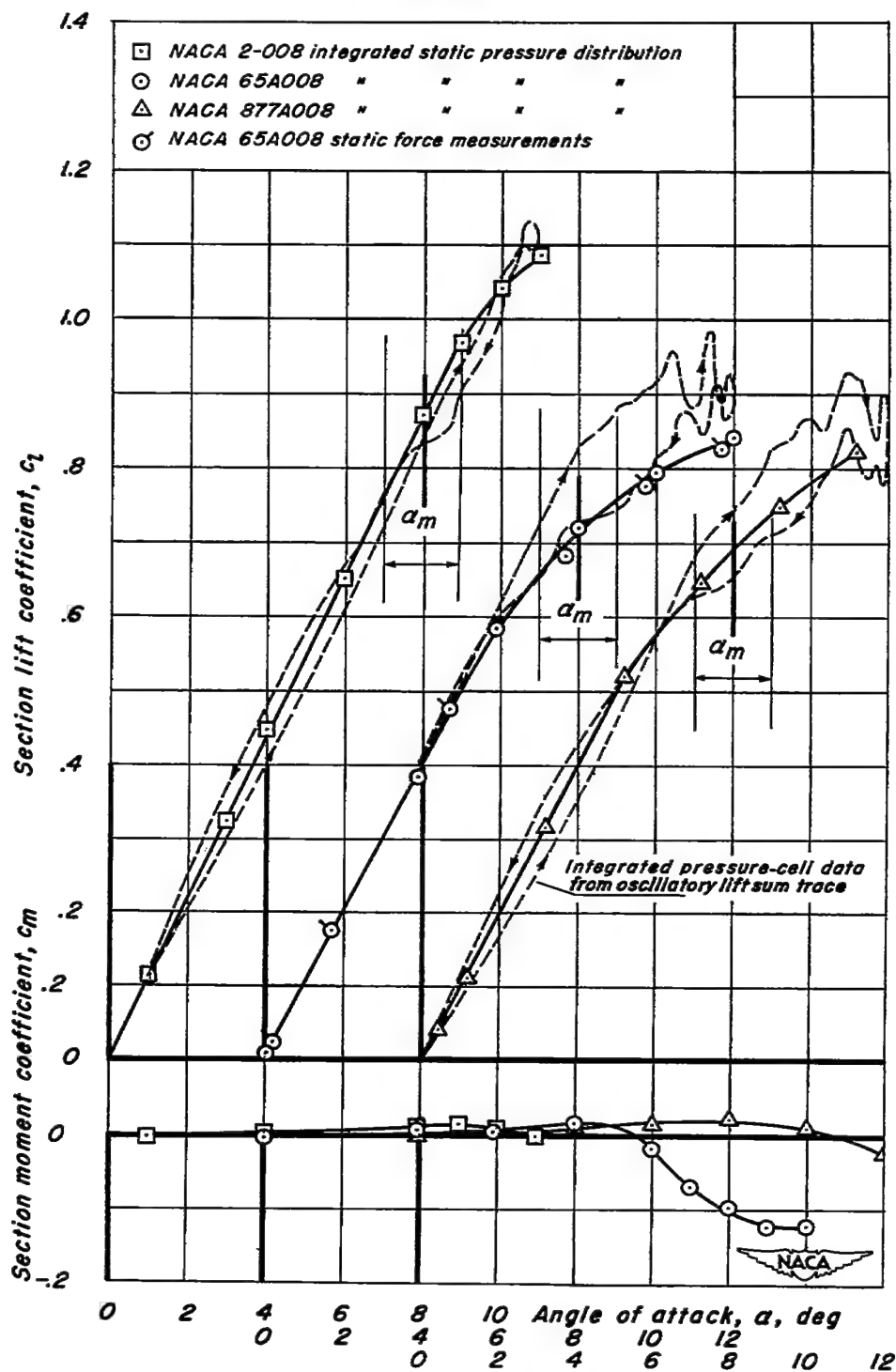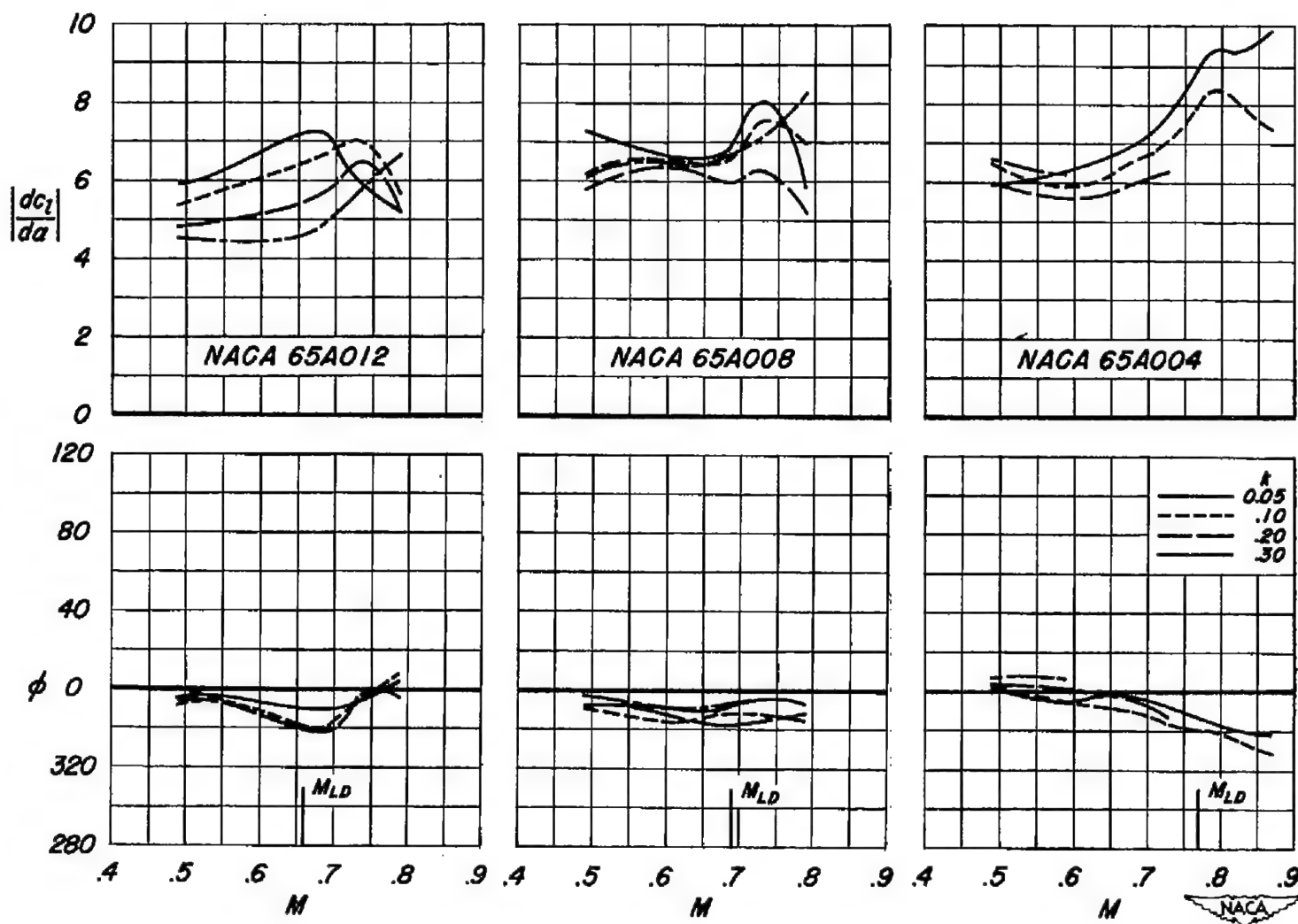
Figure 8.- Concluded.

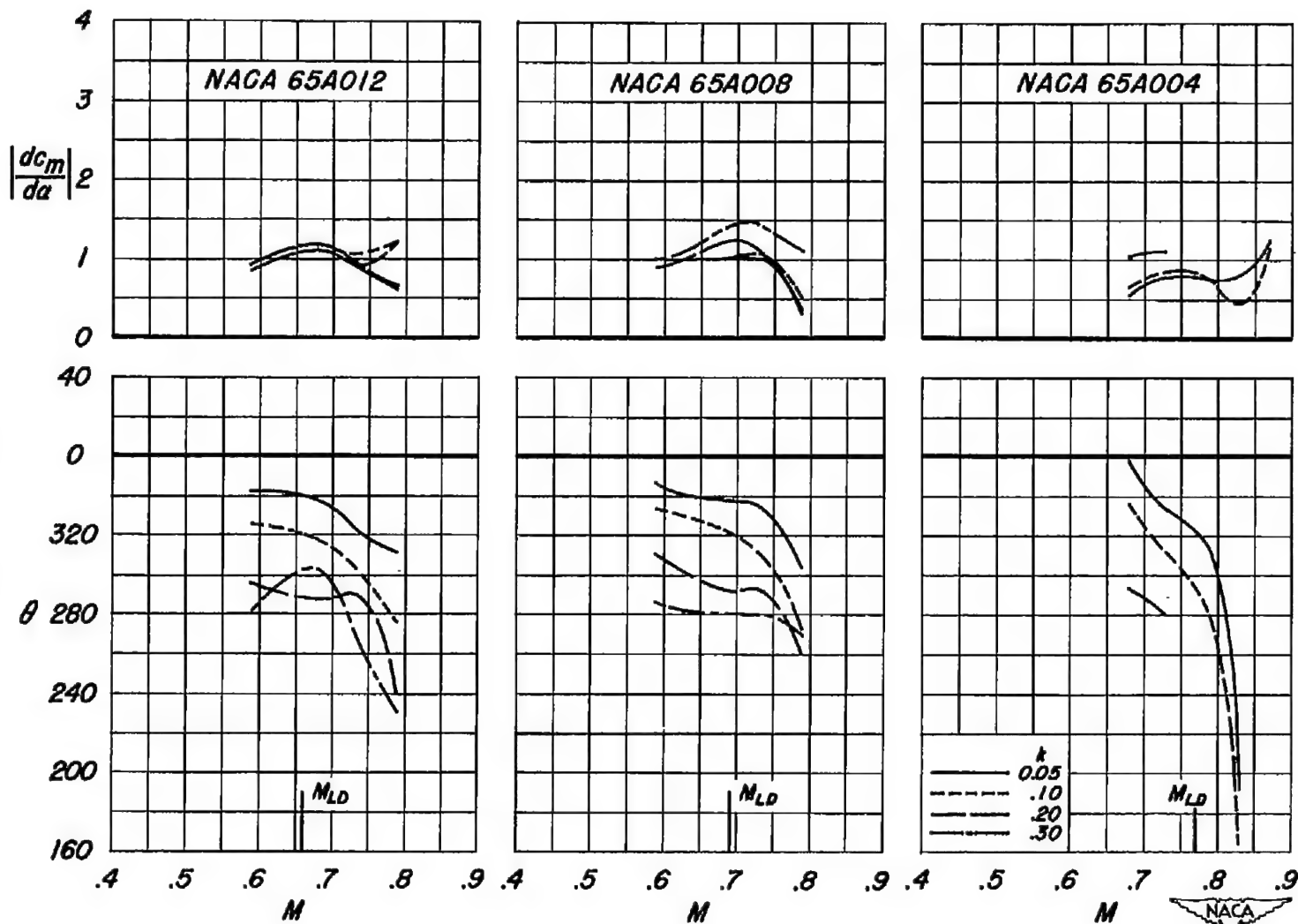(a) Moment derivative and phase angle as a function of
reduced frequency. M = 0.20.

Figure 9.- Effects of airfoil thickness distribution on lift
flutter derivative and phase angle.

(b) Moment derivative and phase angle as a function of
reduced frequency. M = 0.30.
Figure 9.- Continued.

(c) Moment derivative and phase angle as a function of
reduced frequency. M = 0.40.

Figure 9.- Continued.

(d) Moment derivative and phase angle as a function of
reduced frequency. M = 0.50.

Figure 9.- Continued.

(e) Moment derivative and phase angle as a function of
reduced frequency. M = 0.59.

Figure 9.- Concluded.

Figure 10.- Aerodynamic characteristics of the 8-percent-thick airfoils for 0.40 Mach number.

(a) Lift derivative and phase angle.

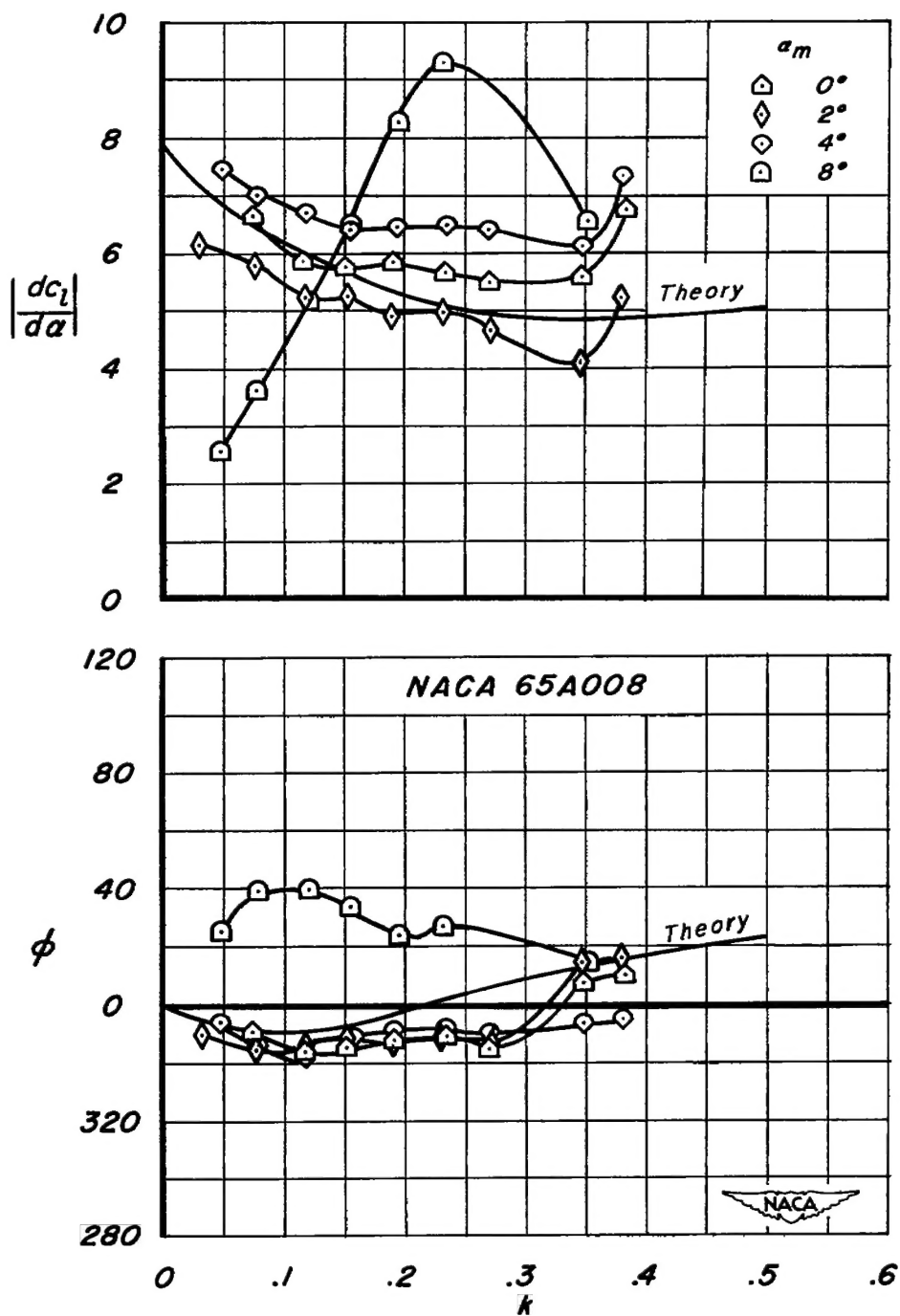Figure II.- Lift and moment flutter derivatives for constant values of reduced frequency as a function of Mach number to show the effects of airfoil thickness. $a_m = 4°$.

(b) Moment derivative and phase angle.
Figure 11.- Concluded.
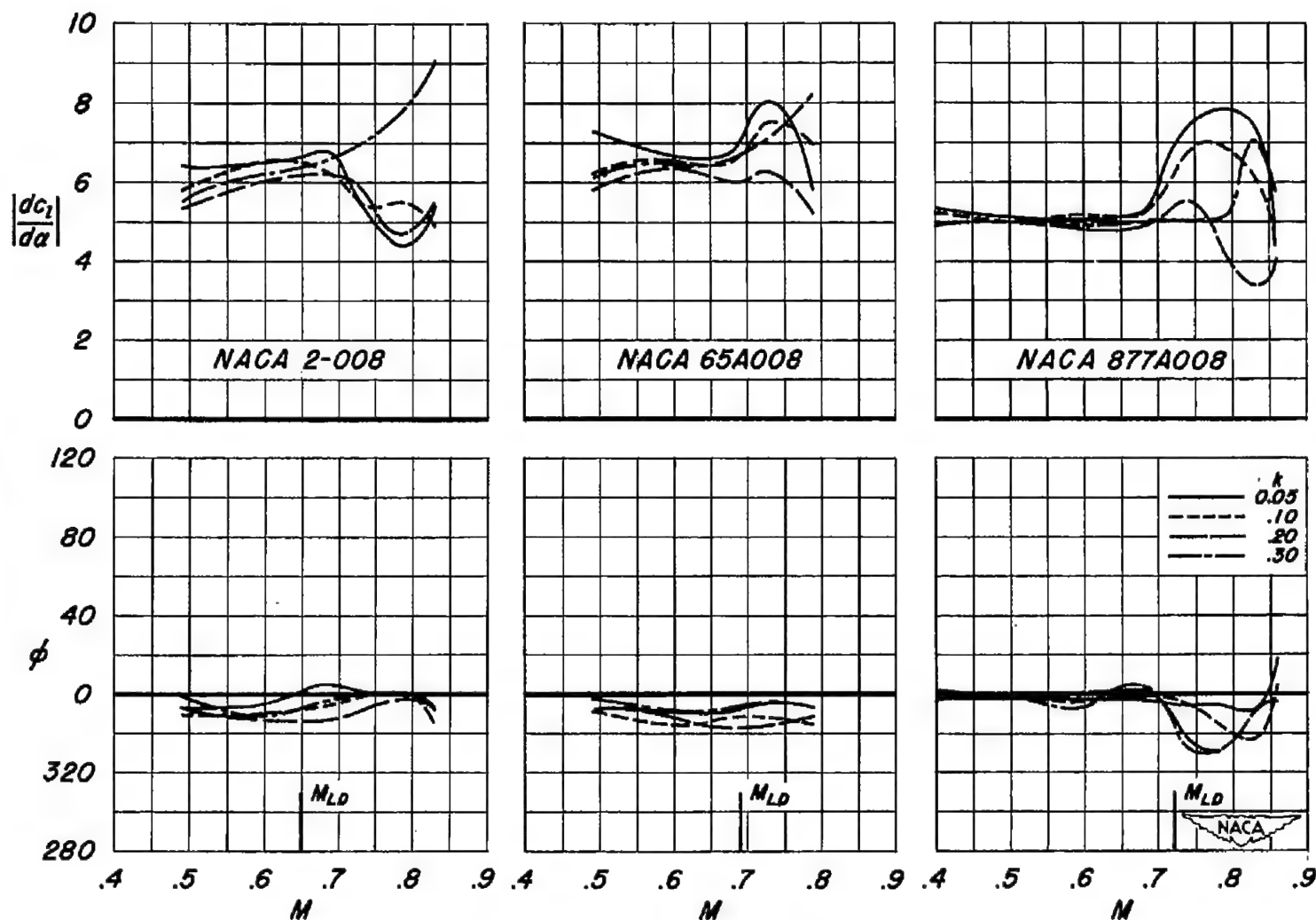
(a) Lift derivative and phase angle.

Figure 12.- Lift and moment flutter derivatives for constant values of reduced frequency as a function of Mach number to show the effects of airfoil thickness distribution. $a_m = 4°$.
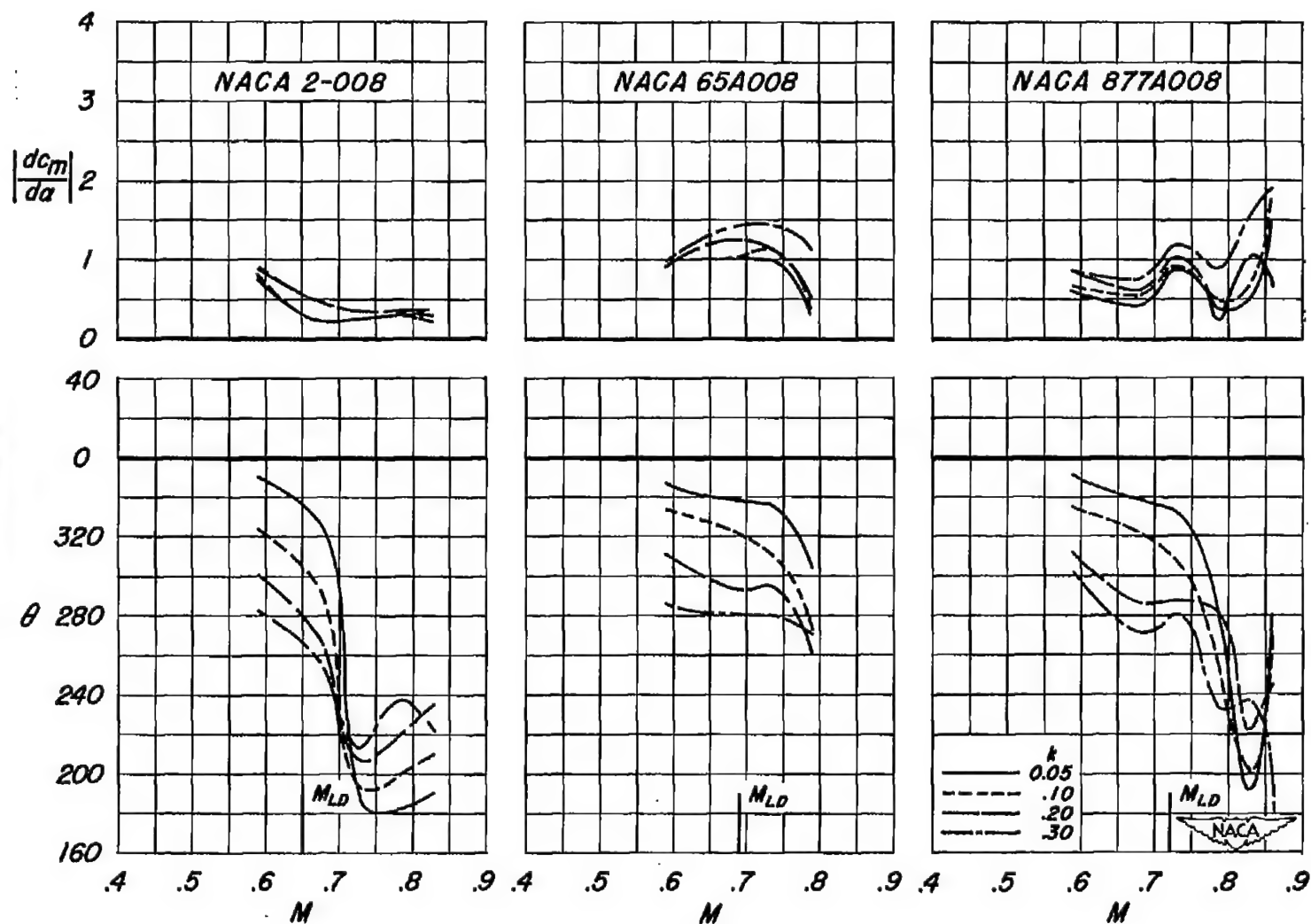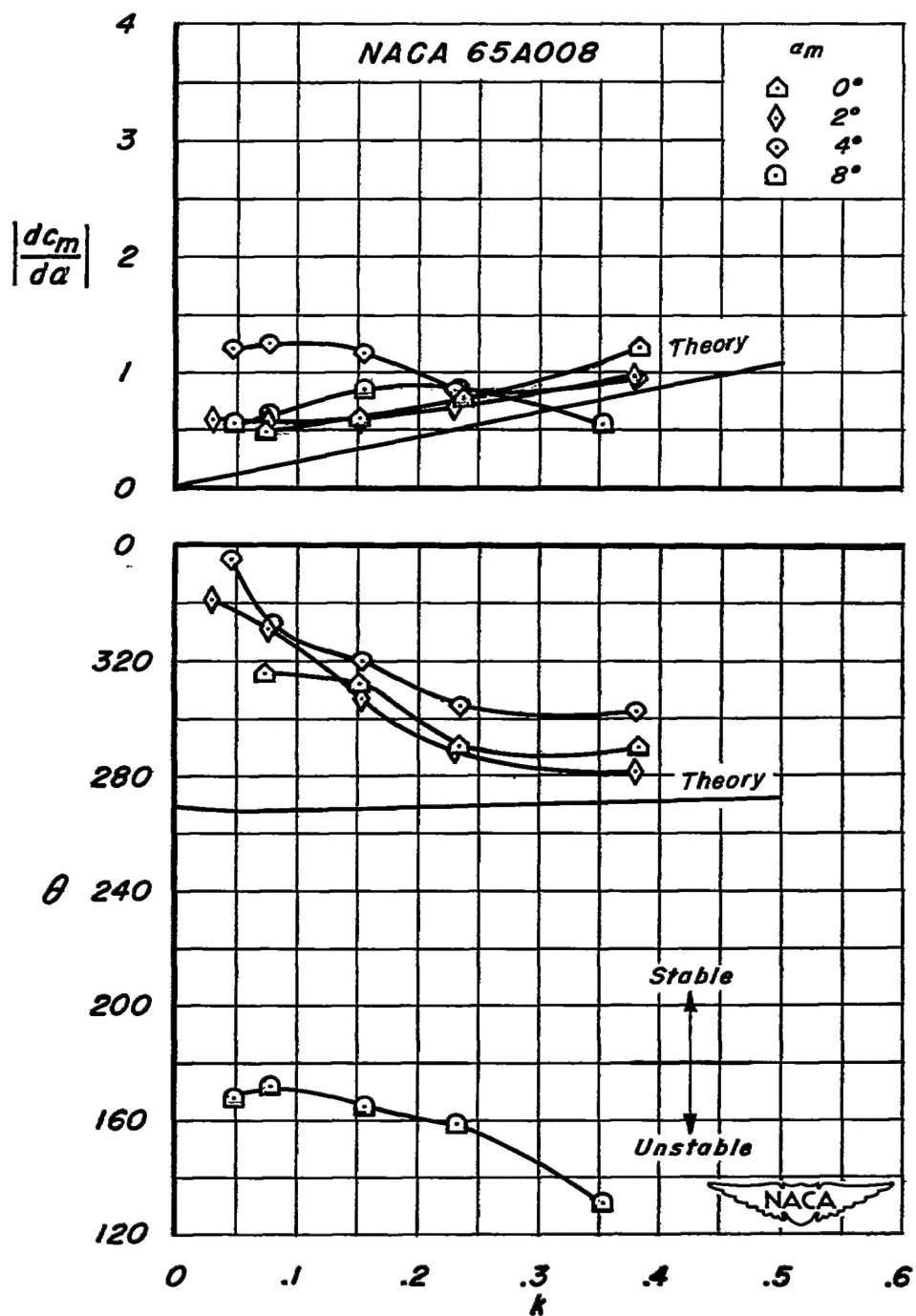
(b) Moment derivative and phase angle.
Figure 12.- Concluded.

(a) Lift derivative and phase angle as a function of
reduced frequency. M = 0.59.

Figure 13.- Effects of angle of attack on the lift and moment
flutter derivatives of the reference airfoil.

(b) Moment derivative and phase angle as a function of
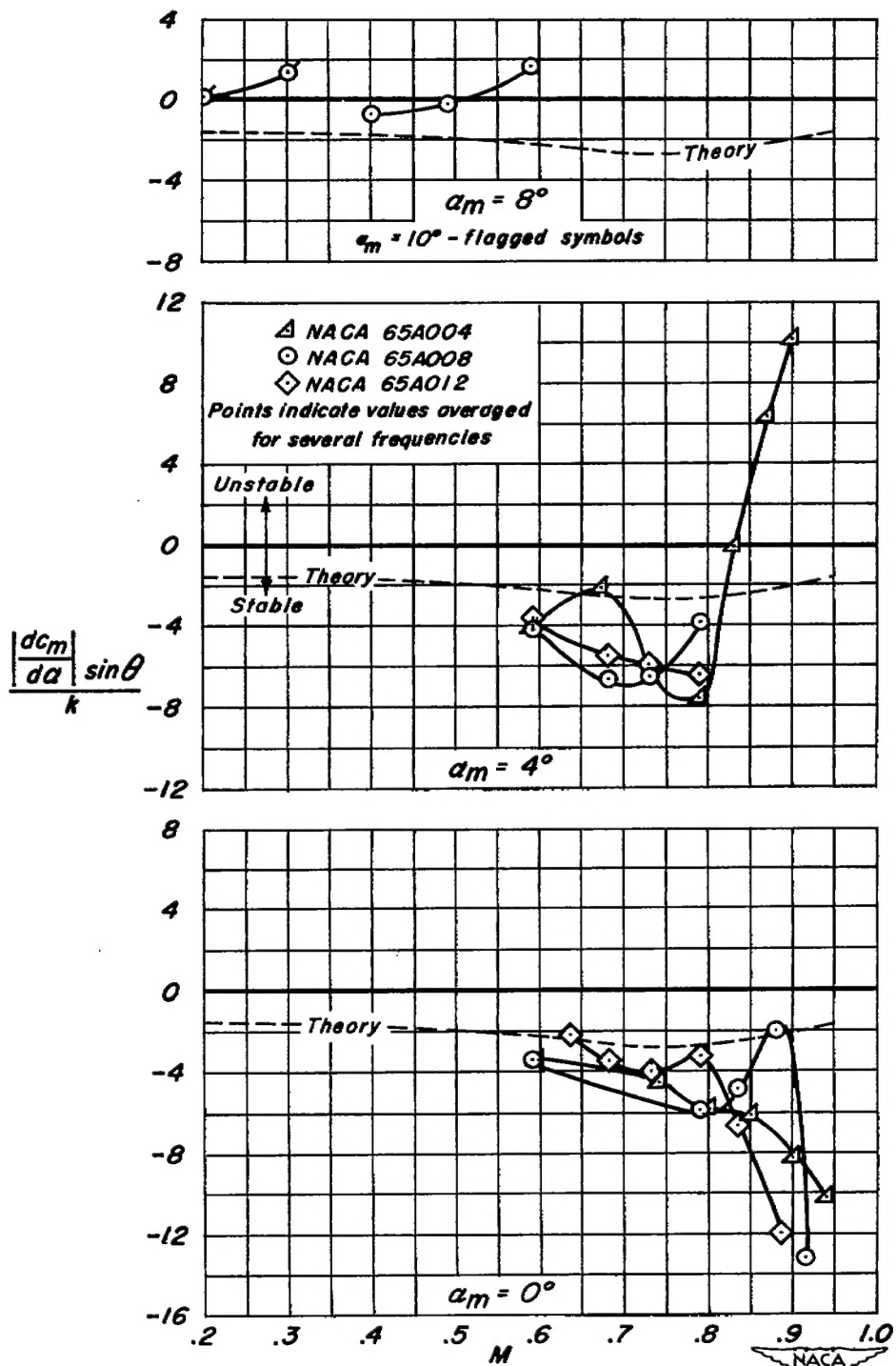reduced frequency. M = 0.59.

Figure 13.- Concluded.

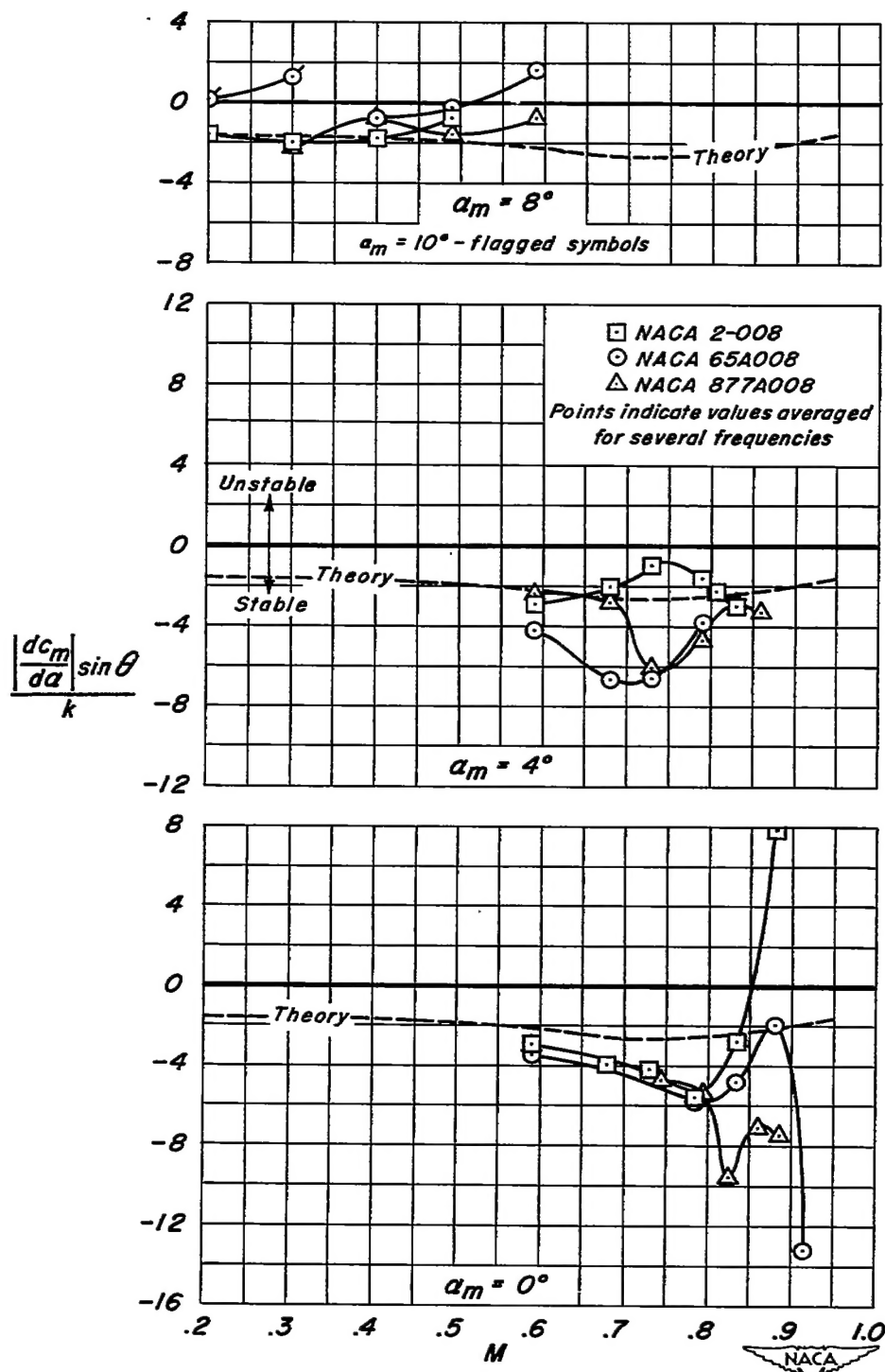Figure 14.- The effect of airfoil thickness on the torsional damping parameter. $\alpha_m = 0°$, $4°$, and $8°$.

Figure 15.- The effect of airfoil thickness distribution on the torsional damping parameter. $\alpha_m = 0°$, $4°$, and $8°$.